M. Sc. Thesis

Physics

Comparison of measurements and water boundary layer model for methane and carbon dioxide fluxes over a boreal lake

Kukka-Maaria Erkkilä

2015

Supervisor: Ivan Mammarella

Reviewers: Ivan Mammarella and Timo Vesala

UNIVERSITY OF HELSINKI

DEPARTMENT OF PHYSICS

PL 64 (Gustaf Hällströmin katu 2)

00014 University of Helsinki

HELSINGIN YLIOPISTO — HELSINGFORS UNIVERSITET — UNIVERSITY OF HELSINKI

Tiivistelmä — Referat — Abstract

Sisävedet (järvet, joet ja purot) ovat kasvihuonekaasujen, erityisesti metaanin (CH_4) ja hiilidioksidin (CO_2) lähteitä. Globaaleissa hiilitaselaskuissa makeiden vesien osuus on usein arvioitu vesirajakerrosmallin mukaan käyttäen kaasunvaihtokertoimen k laskemisessa pelkästään tuulen nopeutta kaasunvaihtoa ajavana tekijänä. Aiempien mittausmenetelmiä vertailevien tutkimusten mukaan tämä malli aliarvioi kasvihuonekaasupäästöjä, eikä sen käyttö ole suositeltavaa luotettavien tulosten saamiseksi. Laajasti järvillä käytetty vuomittausmenetelmä on kammiomenetelmä. Kammioilla saadaan vuomittauksia vain hyvin pieneltä pinta-alalta, joten ne eivät välttämättä kuvaa kattavasti tutkittavaa ekosysteemiä. Kammiomittaukset ovat edullisia ja yksinkertaisia toteuttaa, mutta ne ovat myös työläitä ja mittaukset ovat ajallisesti ja paikallisesti hajanaisia. Tietyn kohdan vuon mittaamisen sijaan nopeat pyörrekovarianssimittaukset (suora vuomittaus, *eddy covariance*) kattavat suuremman lähdealueen. Pyörrekovarianssimenetelmää on laajasti käytetty maa-alueiden vuomittauksissa, mutta niiden suosio järvitutkimuksen parissa on nykyään nousussa.

Tämän tutkimuksen tavoitteena oli verrata pyörrekovarianssi-, kammio- ja rajakerrosmallimenetelmiä CH_4- ja CO_2-vuomittauksissa sekä tutkia niiden ajallista ja paikallista vaihtelua. Mittaukset suoritettiin intensiivisen mittauskampanjan aikana Kuivajärvellä Hyytiälässä (Juupajoki, Etelä-Suomi) syyskuussa 2014. Manuaalisia kammiomittauksia tehtiin neljällä eri mittauspaikalla pyörrekovarianssin lähdealueella 2-3 kertaa päivässä, jotta saatiin tutkittua kaasunvaihdon ajallista ja paikallista vaihtelua. Kaasunvaihtokerroin rajakerrosmallimenetelmää varten laskettiin kolmen eri parametrisoinnin mukaan. Tulokset osoittavat, että rajakerrosmalli korreloi paremmin pyörrekovarianssimittausten kanssa, kun kaasunvaihtokertoimen mallintamisessa käytettiin tuulen lisäksi vesipatsaan konvektion aiheuttamaa turbulenssia. Pelkkää tuulennopeutta käyttävä malli aliarvioi kaasupäästöjä selvästi verrattuna pyörrekovarianssimittauksiin. Kammioilla mitattiin noin 1,7 kertaa suurempia vuoarvoja kuin pyörrekovarianssilla. Vertailu kuitenkin toimii paremmin metaani- kuin hiilidioksidivuolle.

Metaanivuota tarkastellessa huomattiin, että suurimmat vuoarvot on mitattu läheltä rantaa, kun taas hiilidioksidivuossa ei havaittu paikallista vaihtelua. Ajallisesti metaanivuo oli suurin päiväsaikaan, kun järven syyssekoitus oli alkanut. Ennen sekoitusta ei havaittu vuorokausivaihtelua. Hiilidioksidivuossa ajallista vaihtelua havaittiin vain, kun vuo oli laskettu vesirajakerrosmallin mukaan.

HELSINGIN YLIOPISTO — HELSINGFORS UNIVERSITET — UNIVERSITY OF HELSINKI

Tiedekunta/Osasto — Fakultet/Sektion — Faculty	Laitos — Institution — Department
Faculty of Science	Department of Physics

Tekijä — Författare — Author
Kukka-Maaria Erkkilä

Työn nimi — Arbetets titel — Title
Comparison of measurements and water boundary layer model for methane and carbon dioxide fluxes over a boreal lake

Oppiaine — Läroämne — Subject
Physics

Työn laji — Arbetets art — Level	Aika — Datum — Month and year	Sivumäärä — Sidoantal — Number of pages
M.Sc. Thesis	November 2015	47

Tiivistelmä — Referat — Abstract

Freshwaters are a source of carbon to the atmosphere in the form of methane (CH_4) and carbon dioxide (CO_2). Global estimates of the freshwater contribution to the carbon budget are often based on a water boundary layer model (BLM) with gas transfer coefficient k calculated depending solely on wind speed. According to comparison studies, this model gives underestimated emissions and should not be used for more reliable results. A widely used flux measurement method over lakes is the floating chamber (FC) method. FC measures surface flux from a very small area of the lake, so it may not be representative of the whole ecosystem. Measurements are relatively cheap and easy, but also laborious and sporadic. Instead of measuring just a specific point on the lake, eddy covariance (EC) technique provides continuous flux measurements over a much larger source area (footprint). EC systems have been widely used over land areas, but are now growing their popularity in the lake community as well.

The aim of this study was to compare EC, FC and BLM methods for CO_2 and CH_4 fluxes over a boreal lake. The measurements were made at a small dimictic Lake Kuivajärvi in Hyytiälä (Juupajoki, Southern Finland) during an intensive field campaign in September 2014. Manual FC measurements were done at four measurement spots in the EC footprint area 2-3 times a day for catching spatial and temporal variability. Gas transfer velocity for BLM was calculated according to three different parametrizations. Results indicate that BLM fluxes calculated based on water convection and wind driven turbulent gas exchange compare quite well with EC measurements while the model based solely on wind speed is a clear underestimate. FC measurements show about 1.7 times larger flux values than EC. The comparison is more clear for CH_4 than CO_2 fluxes.

The greatest values of CH_4 fluxes were measured near the shore, while CO_2 flux did not show any spatial variability. After the lake started its autumn mixing, CH_4 flux showed a diurnal variation with highest values measured during daytime. There was no diurnal variation before mixing. CO_2 flux on the other hand showed diurnal variation only when calculated according to the BLM method.

Säilytyspaikka — Förvaringsställe — Where deposited
Kumpula Campus library

Muita tietoja — övriga uppgifter — Additional information

Contents

1 Introduction

Global carbon cycle has been widely studied ever since it became obvious that the global warming we are experiencing right now is mainly due to human activities via greenhouse gases, especially carbon dioxide (CO_2). Annual global CO_2 budget estimates have usually included the effects of land and ocean sinks and emissions from fossil fuels, volcanism and land use change (e.g. Houghton et al., 2001; Bernstein et al., 2007) but ignoring the contribution from freshwaters (lakes, rivers, streams and ponds). Lakes release carbon to the atmosphere in the form of CO_2 and methane (CH_4) via turbulent diffusive transfer and CH_4 via emergent aquatic plants and ebullition (MacIntyre et al., 1995). CH_4 is released to smaller extent than CO_2 (Bastviken et al., 2011), but its global warming potential (GWP) is 25 times higher than the one of CO_2 (Bernstein et al., 2007).

Only recently it has been found that also freshwater emissions play an important role in the global carbon cycle (Stocker et al., 2013). Estimates of freshwater contribution and the standard deviation are variable: 1.9 ± 0.5 Pg C yr^{-1} of which 0.11 ± 0.4 from lakes (Cole et al., 2007) or 1.4 Pg C yr^{-1} (of which 0.53 Pg C yr^{-1} from lakes, Tranvik et al., 2009). Raymond et al. (2013) reported global median estimate and its 5% and 95% confidence intervals as $2.1^{+0.77}_{-0.51}$ Pg C yr^{-1} of which $1.8^{+0.25}_{-0.25}$ Pg C yr^{-1} from streams and rivers and $0.32^{+0.52}_{-0.26}$ Pg C yr^{-1} from lakes. The contribution of methane 0.65 Pg C yr^{-1} expressed as CO_2 equivalent has been reported by Bastviken et al. (2011). These latest estimates correspond to about 79% of the annual land sink (2.6 ± 1.2 Pg C yr^{-1}, Stocker et al., 2013) so it can really be said that freshwaters should not be ignored in the global carbon budget calculations.

However, even the biggest estimates might be highly underestimated, since they are based on rough approximations. The most commonly used method for calculating lake greenhouse gas (GHG) emissions is the water boundary layer model (BLM) by Cole and Caraco (1998), which suggests that the gas transfer from lake to the atmosphere is solely dependent on wind speed. Other evaluation methods include e.g. lake-size dependency of wind shear on gas transfer velocity (Read et al., 2012). According to recent studies (Anderson et al., 1999; MacIntyre et al., 2010; Schubert et al., 2012; Heiskanen et al., 2014) this approach gives greatly underestimated

fluxes and gas transfer velocity driving the gas exchange should be further studied for better estimates.

Another widely used flux measurement technique is the floating chamber method (FC). Chambers are cheap and easy to use, which has grown their popularity in the flux community. However, chambers are able to measure surface fluxes only from a very small area, which might not be representative of the whole lake. In addition, there are many sources of uncertainty related to chamber measurements (further discussed in Sect. 2.6.3) and manual measurements are labor intensive. Chamber measurements are sporadic, and usually carried out during daytime. As a result, FC measured fluxes are mostly estimates only for daytime, and the night-time GHG flux might notably differ from this estimate.

The most appropriate currently existing micrometeorological flux measurement method is the eddy covariance (EC) technique. EC flux measurements represent a larger footprint area than e.g. chambers. Measurements are continuous with a high measurement frequency and thus provide information about the temporal variability of the fluxes. EC technique was already developed in the 1950's (Aubinet et al., 2012) and has generally been used over land areas. In recent years, it has however grown its popularity in the lake community as well (Anderson et al., 1999; Eugster et al., 2011; Huotari et al., 2011; Vesala et al., 2006; Schubert et al., 2012; Podgrajsek et al., 2014; Heiskanen et al., 2014; Mammarella et al., 2015). Setting up an EC system over lake requires some considerations related to e.g. prevailing wind direction and meteorological extremes, but once the system is set up, data collection is automatic and the equipment require just a little maintenance once in a while. Although system maintenance is relatively simple, post-processing and filtering EC data is laborious.

There are only few comparison studies between eddy covariance and chambers over lakes (Eugster et al., 2003; Eugster et al., 2011; Schubert et al., 2012, Podgrajsek et al., 2014) and some comparing EC measurements with the BLM method (Anderson et al., 1999; Schubert et al., 2012; Heiskanen et al., 2014). Results from these studies are variable – Eugster et al., 2003 and 2011 measured higher fluxes with chambers than with EC, whereas Schubert et al. (2012) and Podgrajsek et al. (2014) had the opposite result. All studies have had the conclusion that the boundary layer

model is always an underestimate compared to EC.

The main objective of this study was to compare continuous EC fluxes of CO_2 and CH_4 against measurements done by FC and BLM methods. Other objective was to study the diurnal variations of the fluxes. Measurements were made during an intensive field campaign 11.–26.9.2014 at Lake Kuivajärvi in Hyytiälä, Southern Finland. This period was chosen because the lake usually starts its autumn turnover at the end of September. Manual chamber measurements together with water samples were taken from eight different spots on the lake around the EC tower at different times a day for catching temporal and spatial variability of the fluxes. Measurements were performed also during night-time and early morning to catch the effects of night-time convection caused by cooling of the lake surface. Gas transfer velocity k was calculated according to three different models (Cole and Caraco, 1998, MacIntyre et al., 2010 and Heiskanen et al., 2014) and used in the BLM flux calculations to compare with EC measurements. Finally, diurnal variations of fluxes and air concentrations were examined at two different time periods – during lake stratification and mixing period.

2   Theory

In this chapter, the atmospheric boundary layer, the thermal structure and carbon cycle in boreal lakes, and the lake-atmosphere interactions are shortly introduced. Theory of the measurement methods used in this study are then presented in details.

2.1   Atmospheric boundary layer and its diurnal variation

Kaimal and Finnigan (1994) define the atmospheric boundary layer (ABL) as "the region most directly influenced by the exchange of momentum, heat, and water vapor at the Earth's surface". Flow in the ABL is always turbulent, excluding the lowest millimeter (laminar layer), and the turbulent flow consists of eddies of different sizes and velocities. These eddies transport heat, particles, mass and momentum both horizontally and vertically in the atmosphere (called eddy flux). ABL is usually 100–3000 m thick and in its lowest part (about 10% of the thickness, called the surface layer) obstacles have the biggest impact on air flow (Stull, 1988). Vertical fluxes are approximately constant in the well mixed surface layer.

ABL developes right after sunrise when heating of the surface creates convection and turbulent mixing. The well mixed layer grows until it reaches a height of 1–2 km in the afternoon. Thermals that maintain turbulent mixing loose their energy source after sunset and ABL becomes stable. The upper mixed layer then becomes the residual layer and the surface layer shrinks a little bit. Due to radiative cooling, inversion developes in the surface layer and the ABL thickness is now determined by the thickness of the inversion layer (Stull, 1988).

2.2   Thermal structure in boreal lakes

In a stratified lake the water column can be divided into three layers (Wetzel, 2001): mixed surface layer (epilimnion), thin thermocline layer where temperature changes fast with depth, and stable bottom layer (hypolimnion). Epilimnion is the warmest layer during summer and coldest during winter. It is prone to turbulent mixing due to wind. Hypolimnion is the coldest layer during summer and warmest during winter when densest 4°C water sinks to the bottom. Hypolimnion is very stable

and it only mixes during lake turn-over periods (Wetzel, 2001). Thermocline (also called metalimnion) prevents exchange between hypolimnion and epilimnion during stratified periods. When the lake starts cooling down in the autumn, coldest surface water sinks to the bottom of epilimnion and weakens the thermocline. Eventually thermocline disappears and the lake mixes through the whole water column. This brings also gases from the bottom to the surface (Wetzel, 2001). Mixing stops when the lake freezes over and the lake becomes stratified again.

Similar mixing happens also in the spring right after ice-break. As surface water starts warming, it becomes denser than the bottom water and lake turn-over starts. Spring turnover is not as long as in the autumn. It stops when the densest water reaches bottom and the lake stratifies again. Thermocline appears typically in the beginning of June and deepens through summer until mixing starts in autumn.

Dimictic lakes mix twice in a year, monomictic only once (either in winter or summer) and polymictic lakes may mix several times in a year. Boreal lakes are usually dimictic.

2.3   Carbon cycle in lakes

Most lakes worldwide are supersaturated with carbon (Cole et al., 1994), both in the form of CO_2 and CH_4. Boreal lakes contain carbon in three different forms: dissolved inorganic carbon (DIC), dissolved organic carbon (DOC) and particulate organic carbon (POC).

DIC is produced in the lake sediments by decomposition of organic matter and drained from the catchment area, where it has been formed in soil by decomposition and rock weathering. DIC can also dissolve in ground water, from where it drains to lakes. DOC on the other hand is mainly delivered from the catchment area that is rich in carbon (e.g. peatlands). It is also produced in the anoxic lake sediment, but to a lesser extent. POC is produced when primary producers fix DIC to POC, causing seepage of DOC in the process (Hanson et al., 2004). DIC and DOC are additionally formed in the breakdown of POC. POC is partly stored in the bottom sediments, where it is slowly released as DIC to the water column as a product of mineralization.

CH$_4$ is produced through methanogenesis in the anoxic conditions in the sediment, especially in eutrophic lakes, and CO$_2$ formed in the aerobic decomposition of organic matter. In the upper oxic water column, CH$_4$ is likely to oxidize into CO$_2$ (Bastviken et al., 2004). CO$_2$ formation is greater in humic than clear water lakes, but CH$_4$ production is slightly higher in clear water lakes (Ojala et al., 2011).

2.4   Lake-atmosphere interactions

Gas exchange happens between the epilimnion and the atmosphere. Gases are transported to the atmosphere through diffusive transfer in the diffusive sublayer between the surface and turbulent air, by ebullition (which is especially important in the transport of CH$_4$) and by emergent aquatic plants (Fig. 1).

Turbulent eddies transport fluid in the water column and to the water boundary layer (Fig. 1). From the aqueous boundary layer, soluble gases are diffused to the air boundary layer through a 10–100 μm thick laminar diffusive sublayer (MacIntyre et al., 1995) where there is a strong gas concentration gradient. Direction of the diffusive transfer depends on the concentration gradient: diffusion transports gases from higher concentrations to lower. Turbulent eddies in the air then transport gases further in the atmosphere. If the lake is a sink of carbon, then the transport occurs in the opposite direction. This is the main transport mechanism of CO$_2$, since according to Happell and Chanton (1993) even 46% of produced methane gets oxidized into CO$_2$ in the water column before reaching the atmosphere. Importance of the diffusive flux increases with increasing lake surface area (Bastviken et al., 2004).

Bubble ebullition transports gases from the bottom sediments to the atmosphere and is mostly important in the transport of CH$_4$. Production of CH$_4$ in the sediment increases the sum of partial pressures of different dissolved gases above the hydrostatic pressure. This forces dissolved gases to form bubbles and escape the sediment. CH$_4$ content in the bubbles varies from 10% to even 90% (Chanton and Whiting, 1995). When trasported by ebullition, CH$_4$ escapes oxidation in the water column (Happell and Chanton, 1993). Bastviken et al. (2004) estimated that 40–60% of CH$_4$ is released via ebullition and is most important at depths shallower
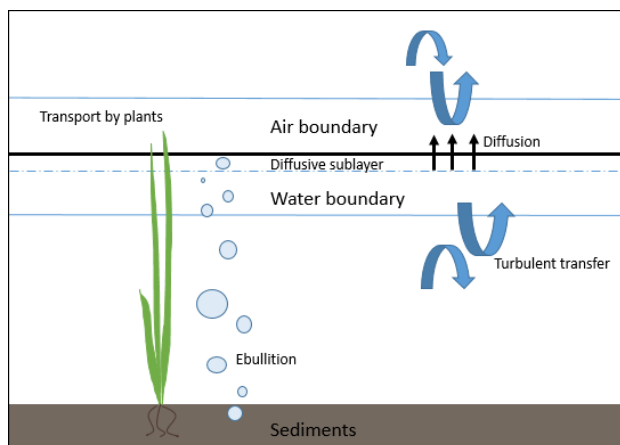
Figure 1. Gas exchange processes. Thick black line represents the air-water interface and thin blue lines air and aqueous boundary layers. The picture is not in scale.

than 4 m. The rate of ebullition is most of all depended on the lake type and depth. Importance of ebullition is still argued because it is very difficult to measure due to its episodic nature (Bastviken et al., 2011).

Gases (especially CH_4) can also be transported to the atmosphere through air-filled hollow tissues in aquatic plants (Chanton and Whiting, 1995). Roots of these aquatic emergent plants usually grow in anaerobic conditions. Therefore plants must provide oxygen for their root respiration from the atmosphere. As a byproduct of this circulation, gases from the sediments get transported to the atmosphere (Chanton and Whiting, 1995). This is again of special importance for CH_4, since also this transport mechanism bypasses oxidation (Happell and Chanton, 1993) and CO_2 is not produced in anaerobic conditions.

2.4.1   Seasonal and diurnal variation of CO_2 and CH_4 exchange

Photosynthesis of algae and aquatic plants decreases the concentration of CO_2 in the surface water during daytime. In the night algae and plant respiration increases the surface water CO_2 concentration. Åberg et al. (2010) also found that diurnal variation in the surface water CO_2 concentration was not necessarily due to photosynthesis but because of wind and upwelling caused by wind. The effects of photosynthesis are lake-dependent and lakes with high primary production are more affected by photosynthesis.

During summer, there might be a diurnal cycle in the CO_2 flux with low values

during daytime due to photosynthesis and high during night-time (Vesala et al., 2006). Vesala et al. (2006) also found that the use of different averaging times in EC fluxes might affect the diurnal variation. A longer averaging period takes into account larger eddies and measurements are more prone to be affected by the surrounding forest. Still not all studies have found a diurnal cycle in the flux itself, only in the air and surface water concentrations (Huotari et al., 2009).

Although summertime fluxes are usually smaller than spring and autumn fluxes (Vesala et al., 2006; Huotari et al., 2009; Ojala et al., 2011; Huotari et al., 2011), Ojala et al. (2011) found that heavy rain events during summertime cause significant peaks in both CO_2 and CH_4 fluxes. Huotari et al. (2011) detected even negative fluxes of CO_2 during summertime due to high primary productivity in Lake Valkea-Kotinen.

A few studies have found a diurnal cycle in CH_4 flux (Podgrajsek et al., 2014; Bastviken et al., 2010; Godwin et al., 2013; Keller and Stallard, 1994) but with variable results. Others suggest higher night-time CH_4 fluxes because of nocturnal convection, while others propose higher daytime fluxes of CH_4 due to wind-induced upwelling.

Seasonal variation of carbon cycling is strongly dependent on the thermal structure and thermodynamics of the lake (Eugster et al., 2003). During stratification periods, the upper mixed layer (epilimnion) is in no contact with the lower hypolimnion and thus gases are transported from bottom to the surface only by ebullition or emergent plants. Lake mixing periods, caused by surface cooling, are the times when most gas fluxes are released. Mixing detaches gases from the bottom sediments and turbulence transports them further in the water column.

2.5 Eddy covariance measurements

EC technique is currently the most accurate and popular flux measurement technique in micrometeorology. Measurements are made in the surface layer of the ABL, where fluxes are constant with height (Sect. 2.1). EC method needs the assumption of homogeneity of the underlying surface and a stationary turbulent flow in the atmosphere (Foken and Wichura, 1996). It is based on fast response instrumentation

measuring vertical wind component simultaneously with the quantity of interest (e.g. dry mole fraction in air). EC system thus consists of a sonic anemometer that measures wind components and temperature, and a gas analyzer.

EC measurements are accurate and continuous with low labour requirements, but the EC system is expensive and it needs extensive data post-processing. For understanding the basics of EC, a few definitions are first needed.

2.5.1 Reynolds decomposition

For understanding the basics of EC measurements, we first have to introduce Reynolds decomposition. Any atmospheric time-dependent quantity can be expressed as a sum of its mean $\bar{f}$ and fluctuating part f':

$$f(t) = \bar{f} + f'(t) \tag{1}$$

where the mean over timeperiod T is defined as

$$\bar{f} = \frac{1}{T} \int_0^t f(t)dt. \tag{2}$$

Now we can introduce Reynold's averaging rules (Stull, 1988):

$$\bar{\bar{f}} = \overline{(\bar{f} + f')} = \bar{f} + \bar{f}'$$

$$\Rightarrow \overline{f'} = 0$$

$$\overline{(\bar{g}f')} = \bar{g}\bar{f}' = \bar{g} \cdot 0 = 0 \; ; \; \overline{(\bar{f}g')} = \bar{f}\bar{g}' = \bar{f} \cdot 0 = 0$$

$$\overline{(f \cdot g)} = \overline{(\bar{f} + f')(\bar{g} + g')}$$

$$= \overline{(\bar{f}\bar{g} + f'\bar{g} + \bar{f}g' + f'g')}$$

$$= \overline{(\bar{f}\bar{g})} + \overline{(f'\bar{g})} + \overline{(\bar{f}g')} + \overline{(f'g')}$$

$$= \bar{f}\bar{g} + \overline{f'g'}$$

where the last term $\overline{f'g'} \neq 0$ is the covariance of the two variables f and g. This is the base of EC measurements, since vertical EC flux is determined by the covariance

of vertical wind component and the quantity of interest (Aubinet et al., 2012). The eddy flux F^{EC} of any gas is defined as

$$F^{\mathrm{EC}} = \rho_a \overline{w'c'} \tag{3}$$

where c is the dry mole fraction of the gas, w the vertical wind speed and ρ_a is the dry air molar density.

2.5.2 Scalar conservation equation

Another equation needed for understanding EC measurements is the scalar conservation equation which describes the conservation of any scalar in the atmosphere (Aubinet et al., 2012). Scalar conservation equation is written as:

$$\frac{\partial \rho_a c}{\partial t} + \nabla(\overrightarrow{u} \rho_a c) = S_c \tag{4}$$

where the first term represents the rate of change of the quantity c, second atmospheric transport and the last term is the source/sink strength of the quantity c. By applying Reynold's averaging rules (Sect. 2.5.1) Eq. 4 can be rewritten as

$$\overline{\rho_a} \frac{\overline{\partial c}}{\partial t} + \overline{\rho_a \overrightarrow{u}} \nabla(\overline{c}) + \nabla(\overline{\rho_a \overrightarrow{u}'c'}) = \overline{S_c}. \tag{5}$$

Eq. 5 assumes that dry air density $\overline{\rho_a}$ is constant with time and states that source term $\overline{S_c}$ equals to the sum of the rate of change of the dry mole fraction, advection in the atmosphere, and divergences in the eddy fluxes (Aubinet et al., 2012). By integrating Eq. (5) over a control volume extending (in vertical direction) from the surface to the measurement height h, dividing with the volume and assuming horizontal homogeneity, constant flux in the surface layer and zero flux at the ground level, we get a simplified estimate of the net ecosystem exchange (NEE)

$$NEE = \underbrace{\frac{1}{h} \int_0^h \overline{\rho_a} \frac{\partial \overline{c}}{\partial t} dz}_{\mathrm{F^{STO}}} + \underbrace{\frac{1}{h} \int_0^h \left(\overline{w \rho_a} \frac{\partial \overline{c}}{\partial z} \right) dz}_{\mathrm{F^A}} + \underbrace{\overline{\rho_a} \overline{w'c'}(h)}_{\mathrm{F^{EC}}} \tag{6}$$

where F^{EC} is the vertical EC flux at height h, described in Eq. 3, F^{A} represents advection of the component c by vertical wind, and F^{STO} is the change of storage of

the scalar between the surface and height h in the atmosphere. If we further assume that there is no net flux of dry air, i.e. $\overline{w\rho_a} = 0$ and also steady state conditions (i.e. partial derivative with respect to time is zero), also the advection F^{A} and storage F^{STO} terms can be neglected and this results to

$$NEE = F^{\mathrm{EC}}. \tag{7}$$

This result suggests that the EC flux term F^{EC} at height h is representative of the NEE in the whole control volume. Hence, surface fluxes may be measured with EC anywhere above the surface, within the atmospheric surface layer.

2.5.3 Other considerations

For measuring relevant scales of eddies, EC instruments need to be fast with a measuring frequency of 10–20 Hz for detecting also the contribution of the smallest eddies and thus improving the flux estimate. Time period used in time averaging the data is usually 30 min for taking into account the contribution of the largest eddies also.

EC method measures fluxes over a source area (footprint) surrounding the flux tower. Footprint area depends e.g. on atmospheric stability, surface roughness and the height of the flux tower (Aubinet et al., 2012).

When considering EC tower installation, a few things should be considered. First, the tower should be placed in a spot that is representative of the ecosystem in interest and with an adequate fetch for the desired wind directions. Second, the tower should be sturdy enough to withstand meteorological extremes of the environment. Third, it should be in a place that is easy accessible for instrument maintenance.

2.5.4 Sonic anemometer and gas analyzers

Sonic anemometers used for measuring wind components at high frequencies are based on measuring the time that it takes for an ultrasound pulse to travel between transducers (Aubinet et al., 2012). The time is dependent on the speed of sound and flow velocity in the air. Air temperature can also be derived from these

13

measurements since the speed of sound is dependent on the air density and thus temperature.

For determining the dry mole fraction fluctuations in air, EC system needs a fast-response gas analyzer, most commonly an infrared gas analyzer (IRGA). IRGA consists of an infrared (IR) light source, detector and band-pass filters for selecting a proper wavelength range for the gases (Aubinet et al., 2012). An infrared light beam is directed to the sample inlet and it is partly absorbed by the gases in the sample. Different gases absorb light at different wavelengths. The remaining IR light is observed at the detector and the observed intensity is a function of gas concentration in the sample (*LI-7200 Enclosed CO_2/H2O Gas Analyzer Instruction manual*).

IRGAs are either closed-path or open-path analyzers. In open-path analyzers, the sample cell is in the open air and thus measurements are affected by ambient conditions and corrections for air density need to be applied. Closed-path analyzers have an internal sample cell and a sampling tube transporting the sample to the analyzer. Fluctuations are damped in the long sampling line and dilution correction needs to be supplied in order to estimate the dry mole fraction. Temperature and pressure are controlled in the sampling line to reduce the need of dilution corrections for H_2O fluctuations (Aubinet et al., 2012).

2.5.5 EC measurements over lakes

When installing an EC system to measure lake-atmosphere interactions, one needs to consider how to mount the tower. EC tower can be installed on a solid foundation on the lake bottom, on the shoreline or on a moored raft. The first two options have the advantage that the mount is sturdy, whereas a raft might be prone to oscillations. On the other hand, a raft might allow more wind directions suitable for EC measurements, depending on the measurement site. When installing an EC system over lake, one must consider extreme wave events, prevailing wind direction and ice breaking, if the system is not taken down during winter.

2.5.6   Sources of uncertainty in EC fluxes

Systematic errors in EC flux measurements usually yield from instrument calibration, data processing issues and assumptions that are necessary for conducting the measurements (Aubinet et al., 2012). Some systematic errors can be corrected using data quality criteria including criteria for e.g. kurtosis, skewness and flux stationarity. Systematic high-frequency attenuation of H_2O can be reduced by cleaning or changing sampling tubes regularly (Mammarella et al., 2009). Moreover, system maintenance and regular calibration of instruments reduces the chances of systematic errors.

Random errors related to EC measurements come from e.g. changes in wind direction and thus effecting the footprint, stochastic nature of turbulence, ability to catch large eddies and instrumental noise (Aubinet et al., 2012).

2.6   Chamber method

Chamber method is based on concentration change inside the closed chamber during the measurement (Livingston and Hutchinson, 1995). Chamber enclosure types are steady-state and non-steady state chambers. In steady-state chambers, air flows through the chamber and the incoming and outgoing airflows are measured. Steady-state chambers have the advantage of constant gas concentration gradient controlling molecular diffusion between the air and the surface. This simplifies flux calculations. Non-steady state chambers have only one sampling port and the gas concentration gradient changes during measurements since there is no flow in and out the chamber. Non-steady state chambers, however, require a much shorter enclosure time than steady-state and are thus less labour intensive (Livingston and Hutchinson, 1995).

Chambers can be vented, meaning that the air inside the chamber is brought to same pressure with the atmosphere. If the chamber is non-vented, fluxes might be underestimated when mass flow from the underlying surface is significant (Livingston and Hutchinson, 1995).

Chamber geometry design depends highly on the measurement site. Especially volume to chamber coverage area ratio, $V : A$, is an important factor when considering the chamber design. Large $V : A$ ratio means that gas concentration change is

more constant, but then the enclosure requires longer sampling intervals (and thus longer measuring times) since the concentration difference is small (Livingston and Hutchinson, 1995). Low $V : A$ ratio causes a more rapid concentration increase in the chamber and allows shorter enclosure times.

Measurement period should be selected on the basis of chamber geometry, study site ecosystem and the gas that is being measured and how much the surface releases the gas. Generally closing time is in the range of 20–40 min (Livingston and Hutchinson, 1995).

When selecting the chamber material, reactivity of the measured gas should be considered. In addition, the material itself should not be a source/sink of the gas.

2.6.1 Floating chamber measurements over lakes

In lake studies, floating chambers (FC) are often used for measuring lake-atmosphere exchange, since chamber method is relatively simple and cheap to use. One major problem with FC measurements is that it disturbs the water-air interface and the measurements are temporally sporadic (Vesala et al., 2006). It can however be used for measuring emissions from a specific place. Floating chambers used over lakes are usually non-steady state, non-vented chambers. Lakes are not as significant trace gas sources as e.g. soils and thus the use of non-vented chambers is justified.

Usually CH_4 emission measurements require a longer enclosing time than CO_2 measurements in lakes because lakes release CH_4 in lesser extent than CO_2 (Bastviken et al., 2011) and the measurement time should be chosen so that the rate of concentration change is constant (Livingston and Hutchinson, 1995). Chamber collar should reach at least few centimeters in water so that waves would not disturb the measurements. On the other hand, collar should not be too much in the water for minimizing disturbances in the gas exchange. Floating chambers also usually have low $V : A$ ratio so that the chamber is more stable on the water and also for ensuring shorter enclosure times.

Air samples should be analyzed as soon as possible after the measurements to prevent outgassing from the container. Usage of glass containers however restrain gases from leaking (Livingston and Hutchinson, 1995).

2.6.2 Chamber flux calculations

After collecting sufficient number of air samples, the samples are analyzed with gas chromatograph. Flux is calculated from the concentration increase in the chamber using equation (Duc et al., 2012):

$$
\begin{aligned}
F &= \frac{\mathrm{d}\chi}{\mathrm{d}t} \frac{pV}{RTA} \\
&= \frac{\mathrm{d}\chi}{\mathrm{d}t} \frac{ph}{RT}
\end{aligned}
\tag{8}
$$

where $\frac{\mathrm{d}\chi}{\mathrm{d}t}$ is the constant concentration increase during the sampling period (μl l^{-1}s^{-1}), p ambient pressure (Pa), V chamber volume (m^3), A the area of the surface that the chamber covers (m^2), R universal gas constant (J mol^{-1}K^{-1}), T ambient temperature (K) and h the height of the chamber (m), defined as $h = \frac{V}{A}$, if the cross-sectional area is constant within the chamber (Livingston and Hutchinson, 1995).

2.6.3 Sources of uncertainty in FC fluxes

Chambers used in this study were manual non-steady state chambers, i.e. samples were collected manually from one sampling line. Therefore, it is clear that the largest random errors come from sampling and processing the samples. Temperature and relative humidity increase inside the chamber does not affect fluxes notably, as reported in Bastviken et al. (2015) and does not need to be taken into account. Samples were collected in glass containers, where there should not be any kind of leakage. If the time between collecting the sample and analyzing it with gas chromatograph is long, there is always the possibility of leakage.

Systematic errors in FC fluxes usually yield from system design and measurement process (Livingston and Hutchinson, 1995). Systematic errors can partly be avoided by choosing the right enclosure design and appropriate closing time. A shorter closing time will reduce temperature increase inside the chamber and decrease the risk of chamber flushing due to waves.

One source of systematic error that cannot be avoided when using FC method

is the disturbance the enclosure causes in the measured surface. It is not yet well known how the chamber affects the surface exchange and so the effects cannot be corrected.

When wanting to measure the ecosystem scale fluxes, the coarsest assumptions in FC measurements of course come from the measurement system itself and whether the measured area is representative of the ecosystem. Manual measurements are also always prone to human mistakes during sampling. These kind of assumptions always increase the possibility of systematic errors.

2.7 Boundary layer model

Boundary layer model describes diffusive gas exchange in the air-water interface discussed in Sect. 2.4. This diffusive flux can be expressed as (MacIntyre et al., 1995):

$$F = \alpha k(c_{aq} - c_{eq}) \tag{9}$$

where F is the surface gas flux, α chemical enhancement factor, k gas transfer velocity (ms^{-1}), c_{aq} the surface water concentration of the gas (mol m^{-3}) and c_{eq} the concentration that the water would have in equilibrium with the overlying atmosphere (mol m^{-3}), defined as

$$c_{eq} = p_c k_H \tag{10}$$

where k_H is Henry's constant (mol m^{-3}Pa^{-1}) and p$_c$ partial pressure of the gas in the atmosphere (Pa).

Generally the chemical enhancement factor α is assumed to be 1 for all non-reactive gases (Cole and Caraco, 1998). Gas transfer velocity k has been modelled by several studies (e.g. Cole and Caraco, 1998; MacIntyre et al., 2010; Heiskanen et al., 2014; Tedford et al., 2014) and its theory is further discussed in the next chapter.

2.7.1 Gas transfer velocity

Gas transfer velocity has been modelled by several studies (e.g. Heiskanen et al., 2014; Tedford et al., 2014; Cole and Caraco, 1998) but still the most frequently used formula is from Cole and Caraco (1998):

$$k_{600CC} = 2.07 + 0.215U_{10}^{1.7} \qquad (11)$$

where U_{10} represents the wind speed at 10 m height (in m/s). The equation is corrected for Schmidt number (Sc) equal to 600, that is k_{600} is the gas transfer coefficient normalized to CO_2 at 20°C. The Schmidt number depends on kinematic viscosity ν and molecular diffusivity D, so that $Sc = \frac{\nu}{D}$. When used in flux calculation, k_{600} should be corrected for local conditions as

$$k = k_{600}\left(\frac{Sc}{600}\right)^{-1/2} \qquad (12)$$

Eq. 11 considers wind speed as the only factor enhancing water turbulence driving the gas exchange between water and air. It has been argued that this might be the case with wind speeds high enough (> 6 m/s, Heiskanen et al., 2014), but several studies have suggested that k is more likely to depend on turbulence at the air-water interface caused by e.g. convective cooling in addition to wind (e.g. Zappa et al., 2007; McGillis et al., 2004; Read et al., 2012; Schubert et al., 2012; Tedford et al., 2014; Heiskanen et al., 2014). Tedford et al. (2014) found a dependency on buoyancy flux β during cooling so that the turbulent dissipation rate ε could be calculated as

$$\varepsilon = \begin{cases} \frac{0.56u_{*w}^3}{\kappa z} + 0.77|\beta| & \text{if } \beta < 0, \\ \frac{0.6u_{*w}^3}{\kappa z} & \text{if } \beta \geq 0 \end{cases} \qquad (13)$$

and the gas transfer velocity then calculated according to the surface renewal model

$$k_{SR} = c_1(\varepsilon\nu)^{1/4}Sc^{-1/2}. \qquad (14)$$

Here $\kappa = 0.4$ is the von Karman constant, z is mixing layer depth (m), here assumed as constant 0.15 m (Heiskanen et al., 2014) and dimensionless constant c_1=0.5 (according to Heiskanen et al., 2014). The friction velocity in the uppermost mm of

the bulk water u_{*w} (Deacon, 1977) is calculated from measurements in the air as

$$u_{*w} = u_{*a}\sqrt{\frac{\rho_a}{\rho_w}} \tag{15}$$

where u_{*a} is the atmospheric friction velocity (m/s) and ρ_w is the water density (kg m^{-3}). Buoyancy flux is calculated as (MacIntyre et al., 1995):

$$\beta = \frac{g\alpha_t H_{eff}}{\rho_w C_p} \tag{16}$$

where g is the gravitational acceleration (m/s^2), α_t the coefficient of thermal expansion (m^{3}K^{-1}), H_{eff} is the effective heat flux (W/m^2), i.e. the sum of latent (LE) and sensible heat fluxes (H), net longwave radiation and the portion of shortwave radiation that is trapped to the mixing layer (Imberger, 1985) and C_p is the specific heat of water (J kg^{-1}K^{-1}). Buoyancy flux is positive when effective heat flux is positive and the lake is heating. If the heat flux is negative, then also buoyancy flux is negative and the lake is cooling.

A new parametrization where k depends directly on both wind speed and buoyancy flux was developed by Heiskanen et al. (2014)

$$k_{Uw_*} = \sqrt{(C_1 U)^2 + (C_2 w_*)^2} Sc^{-\frac{1}{2}} \tag{17}$$

Here $C_1 = 0.00015$ and $C_2 = 0.07$ are dimensionless constants, U is the wind speed above the lake, w_* is the convective velocity defined as

$$w_* = \sqrt[3]{-\beta z_{AML}} \tag{18}$$

and z_{AML} is the depth of the actively mixing layer (m), where temperature varies within 0.25°C of the surface water temperature.

These last two k models need measurements of radiation, heat fluxes, water temperature and air temperature and k_{SR} also air/water turbulence measurements in addition to wind speed. Calculations and measurements are more complicated than in the k_{600CC} model, and this explains the common use of this model.

2.7.2 Sources of uncertainty in BLM fluxes

The most significant source of uncertainty in BLM fluxes comes certainly from the model used for calculating k. We do not know what model is the most accurate and probably none of the existing models is perfect. Therefore, BLM fluxes contain a large uncertainty already in the calculations.

In addition to uncertainties in gas transfer velocity, BLM has other sources of uncertainty as well. For example, measurements for this model are usually taken from one spot and this one spot should be carefully selected for representing the whole ecosystem since surface water concentration may have large spatial variability. In the case of lakes, fluxes from shallower places and near the shore might differ from the ones measured from the middle of the lake. Measurements for the concentration difference $c_{aq} - c_{eq}$ are sometimes taken with manual samples. Manual sampling is always prone to humane mistakes and temporal discontinuity.

Another source of error comes of course from random and systematic errors of the instruments used for measuring gas concentration in air and water. Again, for reducing the error sources, instruments should be cleaned and calibrated regularly.
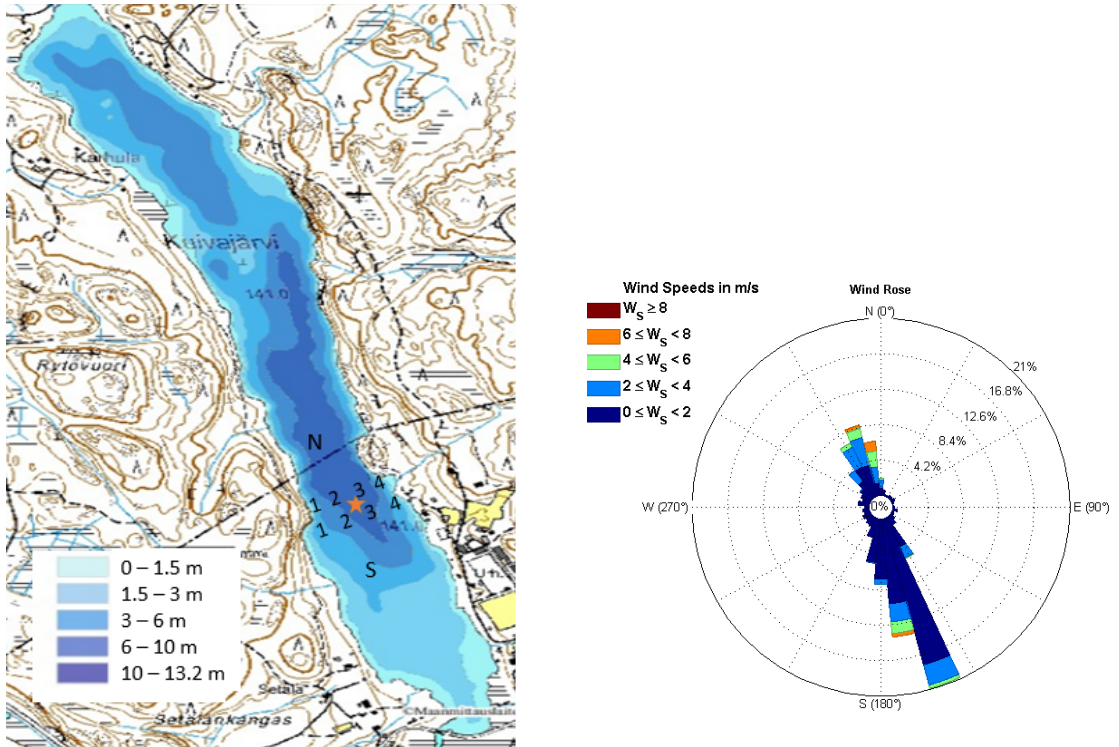
Figure 2. Contour map and wind rose of Lake Kuivajärvi. Orange star points the location of the measurement raft and the numbers 1–4 measurement points of manual measurements both North (N) and South (S) of the measurement raft. Wind rose shows wind direction and wind speed according to their frequency of occurance (shown in percentage) during the measurement period.

3 Measurements and methods

3.1 Site description

Measurements were done in the humic Lake Kuivajärvi which is an oblong lake (Fig. 2) situated in southern Finland (61° 50' N, 24° 16' E) in the middle of a managed Scots pine forest, next to the SMEAR II field station, Hyytiälä. Lake Kuivajärvi is part of the ICOS (Integrated Carbon Observation System) network and the measurements have started already in 2009. It has a maximum depth of 13.2 m, length 2.6 km and width 400 m. The lake has an area of 63.8 ha and it has two separate basins. Wind direction is usually along the lake, as Fig. 2 shows. Measurement raft is situated near the deepest part of the lake in the south basin (Fig. 2).

3.2 Automatic measurements

On the measurement raft on Lake Kuivajärvi there is an EC system at 1.5m above the water surface (Fig. 3). The system consists of a sonic anemometer (Metek USA-1, METEK GmbH, Elmshorn, Germany) for measuring wind speed and its components as well as sonic temperature, an enclosed gas analyzer (LI-7200, Licor Inc., Lincoln, NE) for measuring CO_2 mixing ratio in air and Picarro G1301-f (Picarro Inc., Santa Clara, CA) for measuring CH_4 mixing ratio. Data were collected at 10 Hz sampling frequency and 30 min averaged fluxes were calculated from this data.

CO_2 mixing ratios from the water column were measured at depths 0.2 m, 1.5 m, 2.5 m and 7.0 m with a measurement system consisting of gas-impermeable tubing (stainless steel and teflon), a CO_2 analyzer (CARBOCAP GMP343, Vaisala Oyj, Vantaa, Finland), semipermeable silicone rubber tubing for gas collection (Rotilabo 9572.1, Carl ROth GmbH & Co. KG, Karlsruhe, Germany) and a diaphragm pump (KNF Neuberger Micro gas pump, KNF Neuberger AB, Stockholm, Sweden) for circulating a continuous airstream in a closed loop. Water temperature at depths 0.2 m, 0.5 m, 1.0 m, 1.5 m, 2.0 m, 2.5 m, 3.0 m, 3.5 m, 5.0 m, 6.0 m, 7.0 m, 8.0 m, 10.0 m and 12.0 m was measured using a chain of Pt100 temperature sensors. Air temperature and relative humidity were measured with Rotronic MP102H/HC2-S3 (Rotronic Instrument Corp., NY) and radiation components with Net Radiometer CNR1 (Kipp & Zonen, Delft, Netherlands). These data were collected every 5 s and 30 min averages were calculated.

3.3 Manual measurements

I made manual measurements during the measurement campaign at four different measurement points (Fig. 2), either on the North or the South side of the raft, according to the wind direction to ensure to be on the EC footprint area. Measurement spots were marked with buoys to make sure that the measurements are done always at same locations. Spots were in line so that the closest buoy was at about 50 m distance from the raft. In the middle of the lake (measurement points 2 and 3), the lake depth was about 10 m, and in the points near the shore (1 and 4) the

Figure 3. Measurement raft on Lake Kuivajärvi

depth was about 3 m. I made measurements two or three times a day, depending e.g. on the weather conditions. When the wind speed was high, it was impossible to keep the boat from drifting and thus no reliable manual measurements could be made. Measurements done early in the morning (5 am) or at night (11.30 pm) were performed so that we would catch the nocturnal water convection. Measurements in the afternoon would catch the strongest wind induced turbulence.

FC measurements were made so that the closing time of the chambers was 20 min with a 5 min measuring interval. All measurements were performed using two replicate plastic buckets that were surrounded with Styrofoam floats (Fig. 4). Chambers were covered with reflective aluminium tape and they had a volume of 7.5 l and height above water 9.6 cm. Chambers reached approximately 3 cm into the water. Air samples were taken by syringes that were pumped for 30 s before sampling to mix the air inside the chamber and to clean the syringe. Two 30 ml surface water samples were also taken from each spot.

After all measurements were done, the samples were processed in the lab. Air samples were injected into 12-ml Labco Exetainer ® vials (Labco Ltd., Lampeter, Ceredigion, UK) after flushing them with 30 ml of the sample.

Water sample syringes were filled with 30 ml of nitrogen and put in a water bath

Figure 4. Manual FC measurements from a boat.

with a constant temperature of 20°C. After 30 minutes had passed, the syringes were shaken vigorously for 3 minutes to separate the dissolved gases from the water to the nitrogen gas. After this, the nitrogen mixture was carefully injected to pre-evacuated 12-ml Labco Exetainer ® vials.

Overpressurized vials were then analyzed with a gas chromatograph. The system consisted of a Gilson GX-271 Liquid handler (Gilson Inc., Middleton, WI, USA), a 1-mL Valco 10-port valve (VICI Valco Instrument Co. Inc., Houston, TX, USA) and an Agilent 7890A GC system (Agilent Technologies, Santa Clara, CA, USA) equipped with a flame- ionization detector (temperature 210°C).

3.4   Data processing

3.4.1   Processing of EC data

For EC flux calculation and data processing I used EddyUH software (https://www.atm.helsinki.fi/Eddy_Covariance). Spikes in the data were removed on the basis of a maximum difference being allowed between two adjacent points. Limits for difference between subsequent data points were defined to be 10 m s^{-1} for u and v, 7 m s^{-1} for w, 5 °C for sonic temperature Ts, 50 ppm for CO_2 mixing

ratio, 5 mmol mol^{-1} for water vapor mixing ratio and 10.5 ppm for CH$_4$ mixing ratio.

Linear trend was removed from the background of turbulent fluctuations using linear detrending option, and 2D coordinate rotation was done so that the wind component u is directed parallel to the mean horizontal wind, and the mean of the other wind components is zero ($\bar{v}$=0 and $\bar{w}$=0).

Closed-path measurement system often causes the CO$_2$, CH$_4$ and water vapor cospectrum to decrease before temperature cospectrum at high frequencies. This high-frequency attenuation results in underestimation of fluxes (Aubinet et al., 2012) and should be corrected using transfer functions. In this study, high frequency spectral corrections were calculated according to Horst (1997). Response times that describe the system performance at high frequencies were used in the calculation: 0.2 s and 0.3 s for CO$_2$ and CH$_4$, respectively.

3.4.2   Quality criteria

I cleaned the data so that unphysical data points were removed. Limits for gas mixing ratios were for CO$_2$ 360<[CO$_2$]<500 ppm, for CH$_4$ 1.5<[CH$_4$]<2.5 ppm and for water vapor 0.1<[H$_2$O]<50 mmol mol^{-1}. If the second angle of coordinate rotation was greater than 10°, data from that period was ignored. Data with flux stationarity FST>1, skewness |Sk|>2, kurtosis Ku<1 or Ku>8 were deleted to improve data quality (Vickers and Mahrt, 1997). Wind directions other than along the lake were ignored to avoid fluxes coming from the forest. The approved wind directions were 130°<WD<180° and 320°<WD<350° (Fig. 2). For CO$_2$ flux, also a criteria for standard deviation of CO$_2$ mixing ratio was used. During nighttime, the standard deviation often increased indicating that there was advection of CO$_2$ from the forest to the lake which causes scatter in the flux measurements. From the data it was obvious that this scatter is small when the standard deviation of CO$_2$ is less than 3. CO$_2$ data with standard deviation larger than 3 were removed. After all processing procedures, the data coverage were 27% and 53% of the original data for CO$_2$ and CH$_4$, respectively. EC footprint reaches 100–300 m from the raft, depending on the stability conditions (Mammarella et al., 2015).

3.4.3 FC flux calculations

Concentration increase in the chamber was clearly linear. The flux was calculated from the slope of the linear fit using Eq. 8 and accepted if the coefficient of determination r^2 was at least 0.90. Pressure data for flux calculations were taken from SMEAR II station nearby and temperature data from the meteorological measurements on the raft. CO_2 flux was assumed to be zero if concentration change inside the chamber was small (less than 40 ppm) during the 20 min enclosure time.

3.4.4 BLM flux calculations

In BLM calculations, k parametrizations from three different studies (Cole and Caraco, 1998, Tedford et al., 2014 and Heiskanen et al., 2014) were used and the calculations are explained in detail in Sect 2.7.1. CO_2 concentration in air was measured with enclosed gas analyzer (LI-7200, Licor Inc., Lincoln, NE) of the EC system and surface water concentration was taken from Vaisala CO_2 analyzer described in detail in Sect. 3.2. Pressure data were taken from SMEAR II station and temperature, wind speed, H, LE and radiation were measured at the measurement raft.

# 4 Results and discussion

4.1 Meteorological conditions and water profile measurements

Weather was warmer than usually in September 2014 during the measurement campaign, with a maximun air temperature of 18.5°C on 11.9 (Fig. 5a). Lowest temperature 0.12 °C was detected on 24.9. Surface water was also quite warm, 17.6 °C at highest in the beginning of the campaign, and 10.8 °C at lowest in the end of the campaign.
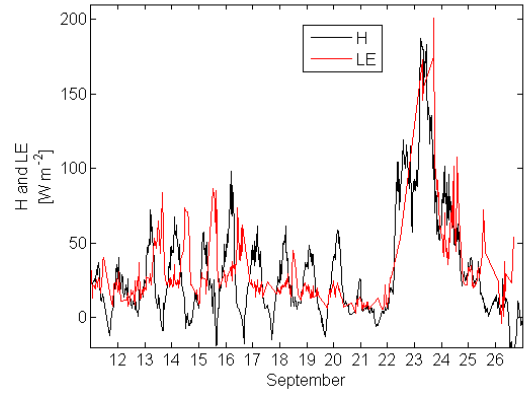
Sensible heat flux was mostly positive (i.e. from the lake to the atmosphere) as usually in the fall when water temperature exceeds air temperature (Fig. 5b). Sensible heat flux was highest during night when the water was warmer than air above. Latent heat flux was the same magnitude as sensible heat flux. This is not expected over large water basins but the result is reasonable over Lake Kuivajärvi since it has relatively small area. Latent heat flux gained highest values at daytime when the sun gave the most energy for evaporation and the temperature difference between air and water was not as large as during night (i.e. energy was not used for sensible heat flux). Both heat fluxes increased drastically to about 190 Wm^{-2} on 22.9. This is probably due to high wind speed (Fig. 5c) and low air temperature resulting from north winds (Fig. 5d) enhancing the heat exchange between water and air.

During the campaign there were only two days with heavy rain (Fig. 5e). Sun rised between 6:30–7:15 am and set between 7:10–8:00 pm during the campaign. Shortwave radiation is presented in Fig. 5f and it clearly shows cloudy days and approximately sunrise and sunset times.

Water column was thermally stratified the first 11 days of the campaign when the thermocline was at about 7.5 m depth (Fig. 6), and the well mixed surface layer was approximately 5–6.5 m deep. Sudden drop in temperature due to north wind (Fig. 5d), high wind speed (up to 7.6 m/s, Fig. 5c) and heavy rain (11.1 mm/d, Fig. 5e) however triggered mixing in the water column on 22.9. The mixing only occured until 8 m and later until 11 m depth (Fig. 6).
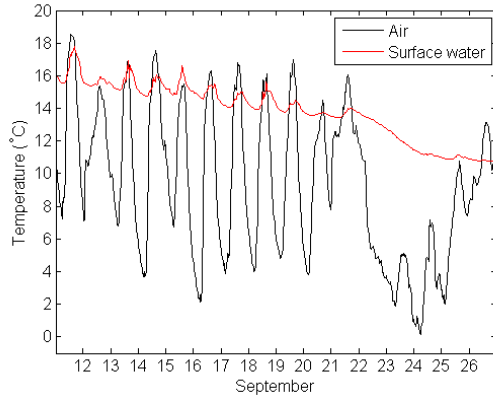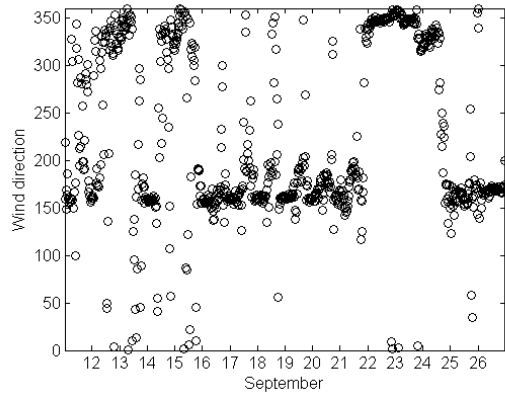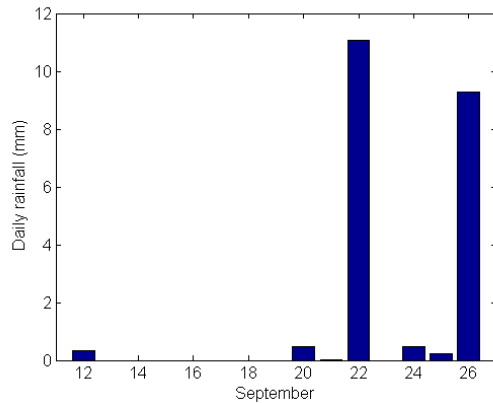
(a) Air and surface water temperature (°C)   (b) Sensible and latent heat flux (W m^{-2})
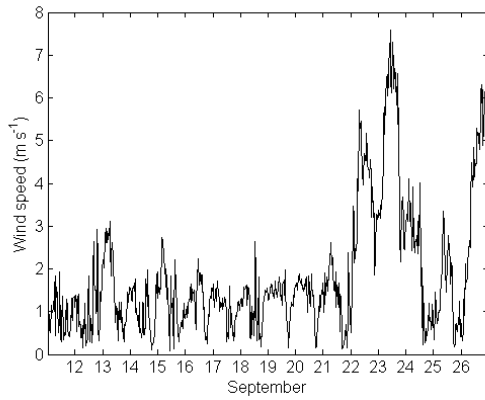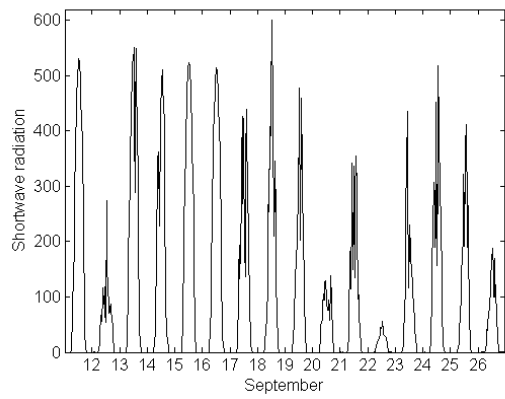
(c) Wind speed (m s^{-1})   (d) Wind direction (°)

(e) Daily rainfall (mm)   (f) Incoming shortwave radiation (W m^{-2})

Figure 5. Meteorological data in September 2014. Dateticks represent midnight.

On 14.9 the well mixed surface layer deepened from 5 m to 6.5 m (Fig. 6). At this time also CO_2 concentration at 7 m decreased to 2900 ppm for some time, indicating that some gases were released to surface water and to the atmosphere (Fig. 7). This is also seen in the manual surface water measurements of CO_2 (Fig. 8a) as the concentration seems to drastically increase from 2100 ppm to even 11400 ppm in all measurement points during 14.–15.9. Highest CO_2 surface water concentration 11400 ppm was measured at measurement point S4, i.e. near the shore on the south side of the raft on 14.9. CH_4 concentration in the surface water increased from around 2 ppm to 3 ppm for the period 16.–20.9 (Fig. 8b) in all measurement spots. That time there was no increase in CO_2 concentration and it is possible that CH_4 concentration increased due to ebullition. CH_4 concentration in the surface water increased drastically after mixing started reaching values of even 10.2 ppm. On 17.9 the well mixed surface layer reached 6.5 m depth causing a slight increase in the surface water CO_2 concentration, while concentration at 7 m depth decreased (Fig. 7). Concentration gradient in the first 7 m of the water column almost vanished on 22.9 when the lake started mixing. However, mixing did not reach the bottom and probably only a small amount of CO_2 rich water rose from the deep. This would explain why the surface water concentrations do not show that clear increase in Figs. 7 and 8a.

4.2   FC and EC flux comparison

Time series of the measured CH_4 and CO_2 fluxes are presented in Fig. 9. There are no manual FC measurements during the very windy period 22.-25.9 because it was impossible to keep the boat from drifting.

The CO_2 gas analyzer broke down at the end of the campaign (25.9) and therefore we do not have EC measurements of CO_2 flux from the last two days.

4.2.1   Methane flux comparison

EC fluxes of CH_4 are very close to zero before the autumn mixing (Fig. 9a). It varies around zero because the CH_4 flux is very close to the Picarro analyzer's detection limit (2 nmol m^{-2}s^{-1}, Peltola et al., 2014). FC fluxes measured at different locations
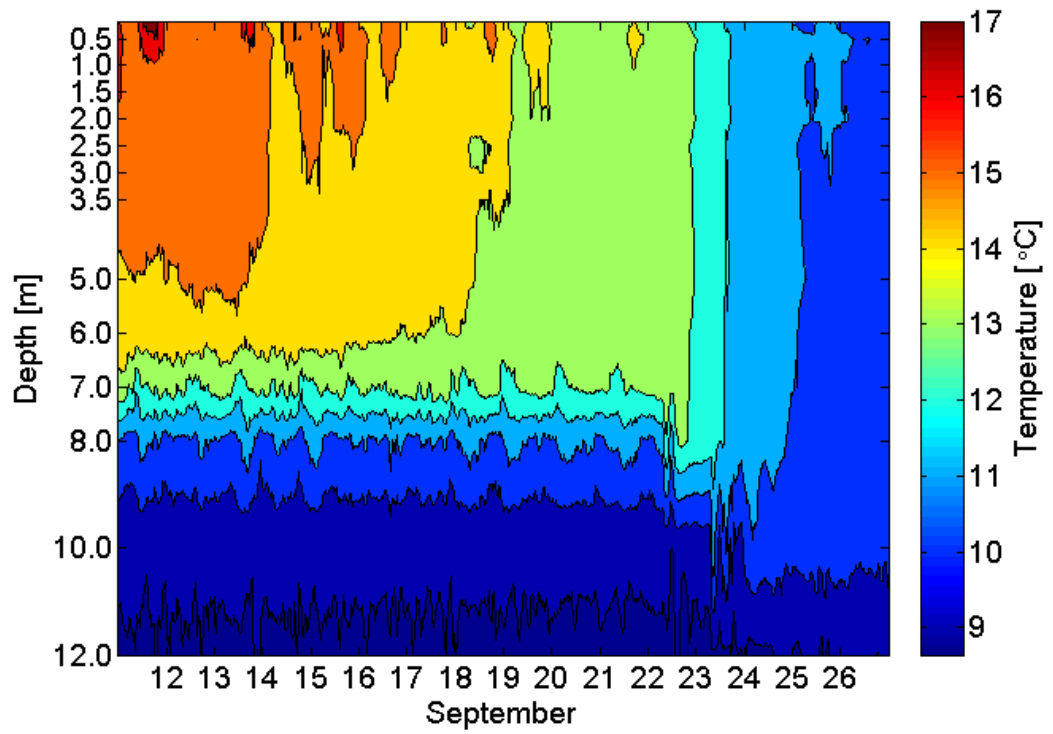
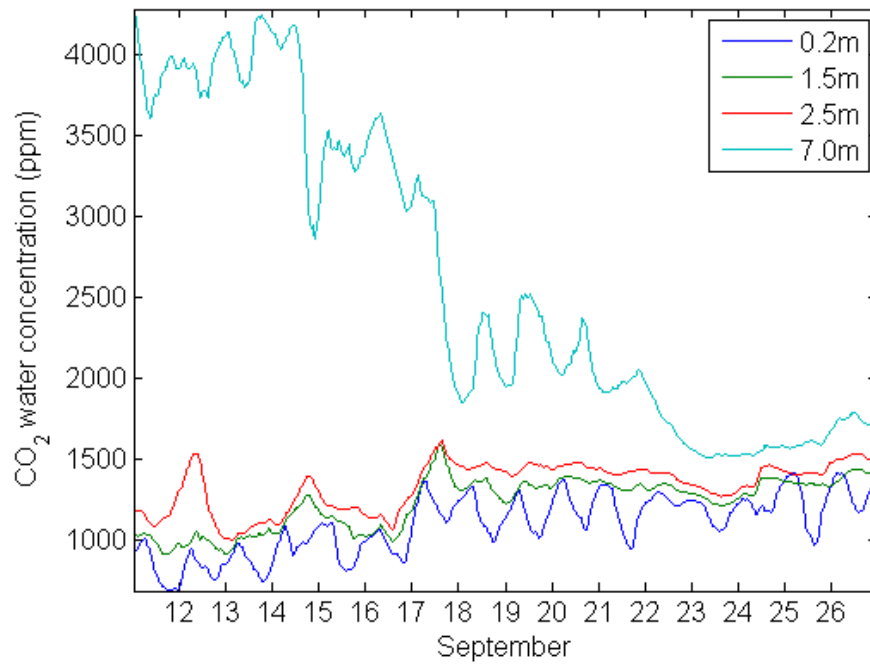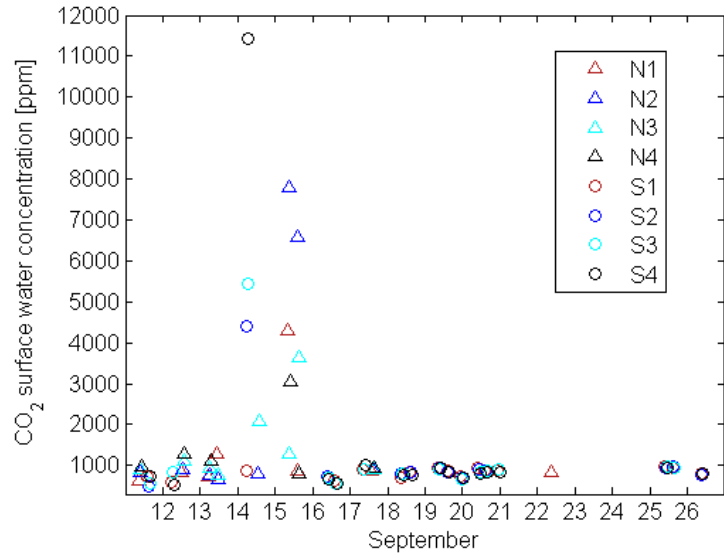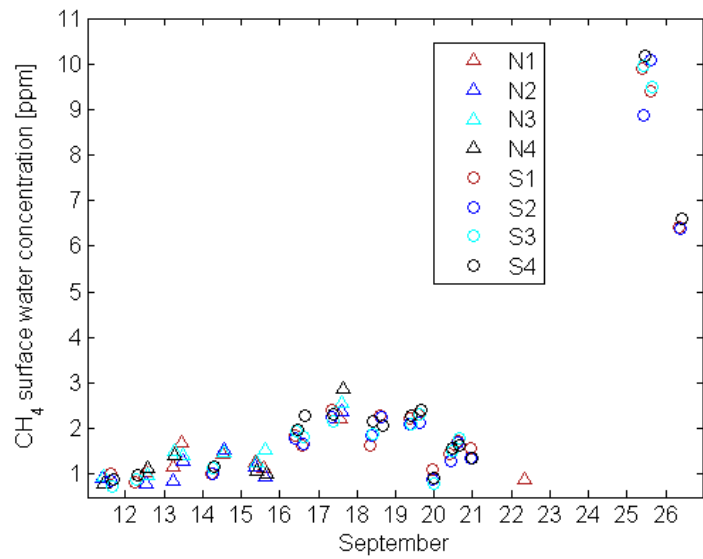Figure 6. Temperature profile in the water column.

Figure 7. CO$_2$ concentration in the water column.

(a) CO_2 surface water concentration.

(b) CH_4 surface water concentration.

Figure 8. Surface water concentrations of CH_4 and CO_2 taken from manual samples at different measurement locations. N1 represents the measurement spot near the shore, north from the measurement raft (Fig. 2)

show that before autumn mixing all distinguishable higher fluxes were measured near the shore (red and black triangles and circles in Fig. 9a), where CH_4 production is higher than in the middle of lake (due to higher sediment temperature) and also oxidation is not as likely as in the deeper parts of the lake. The highest FC flux before mixing (12 nmol m^{-2}s^{-1}) was measured on 15.9 at measurement spot N4, i.e. near the shore at the north side of the measurement raft (Fig. 9a). In the very windy period, 22.–25.9, EC fluxes were really high due to enhanced gas transfer accross the water-air boundary. FC measuremets have a gap during this period because of too high wind speeds disturbing the manual measurements. Maximum CH_4 flux was measured both with FC (13 nmol m^{-2}s^{-1}) and EC (16 nmol m^{-2}s^{-1}) when the mixing had started in the end of the campaign. In this period, highest chamber fluxes were measured at the middle of the lake, where water with high CH_4 concentration welled from the bottom due to mixing (Fig. 8b).

FC measurements are compared against simultaneous EC measurements in Fig. 10a. It is clear that FC fluxes are usually higher than EC fluxes. This was also the result that Eugster et al., 2011 found in their study. Podgrajsek et al., 2014 and Schubert et al., 2012 on the other hand found that the cumulative CH_4 flux was greater when measured with EC than when measured with FC. The highest overestimations come when the flux is measured near the shore or during the mixing period. As a conclusion, CH_4 is released more in shallower areas and thus measurements near the shore are not directly comparable with EC measurements over a larger area.

4.2.2 Carbon dioxide flux comparison

As opposed to CH_4 flux measured with chambers, CO_2 chamber flux does not show observable spatial variability (Fig. 9b). Chamber CO_2 flux is always positive or zero and there is no noticeable increase after mixing started expect on day 22.9, when the FC flux is very close to the average EC flux. EC measurements show a clear increase after 22.9, when the average flux reached even 1.7 μmol m^{-2}s^{-1} in the end of the campaign. EC flux on average is mostly positive, aside from two few hour occasions in the beginning of the campaign. Maximum FC CO_2 flux was measured at measurement spot S3 (in the middle of the lake on the south side of the raft) on

16.9 (2.3 μmol m^{-2}s^{-1}) and with EC on 23.9 (7.6 μmol m^{-2}s^{-1}). During days 15.–16.9 also surface water concentrations were highest, as Fig. 8a shows. This might indicate that there was some local upwelling causing deeper water to rise upwards, although we do not see this kind of behaviour either in the CH$_4$ FC flux nor in the surface water concentrations of CH$_4$ (Figs. 9a and 8b, respectively). It could also be that CH$_4$ has oxidized to CO$_2$ on its way to the surface, causing CO$_2$ concentration in the surface to increase. EC measures the flux from its footprint area and would quite possibly miss this kind of local upwelling occasions.

As for CH$_4$, also CO$_2$ EC fluxes show high positive values during the windy period 22.-25.9 when the lake started mixing due to enhanced gas exchange.

FC measurements of CO$_2$ are compared against EC measurements in Fig. 10b. FC measurements are mostly showing larger values compared to EC measurements, but for CO$_2$ this comparison is not as clear as for CH$_4$, since there are also periods when EC is clearly higher than FC flux. As a conclusion, for CO$_2$ fluxes the results of this method comparison are less clear than for CH$_4$. Podgrajsek et al. (2014) found similar results in their method comparison study, but also stated that the reasons for this are not clear at the present.

In the end, FC and EC measurements are not quite comparable with each other. EC measures the flux over a large footprint area while FC measures fluxes only from its cross-sectional area. In addition, floating chambers disturb the air-water interface and might cause some bias in the measurements by generating turbulence in calm conditions (Vachon et al., 2010). In summary, EC does not count for local upwelling periods and is more representative of the lake than the spot measurement. Chambers on the other hand are very useful for measuring specific places of the lake, e.g. near the shore, where EC measurements would not work that well.

4.3   BLM and EC comparison of CO$_2$ flux

EC and BLM fluxes with k calculated according to Heiskanen et al. (2014), Tedford et al. (2014) and Cole and Caraco (1998) are represented as a time series in Fig. 11. The time series shows that the newest k models (Heiskanen et al., 2014 and Tedford et al., 2014) give quite similar results to the mean EC flux. Model by
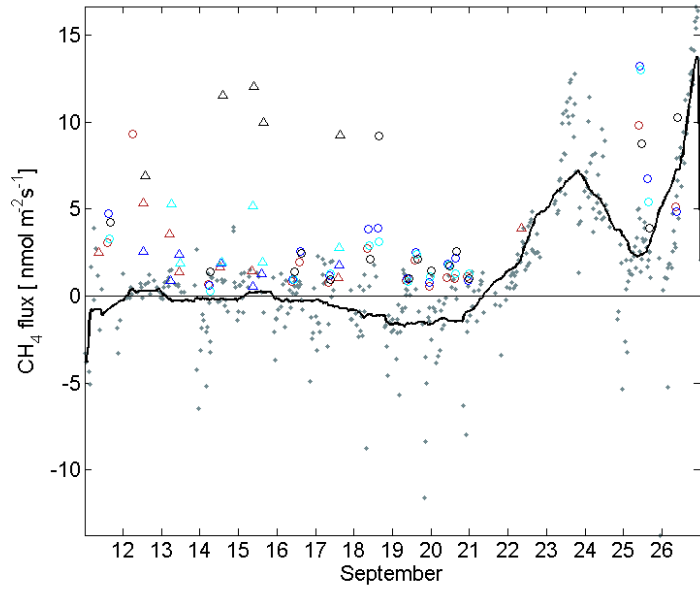
(a) CH$_4$ flux
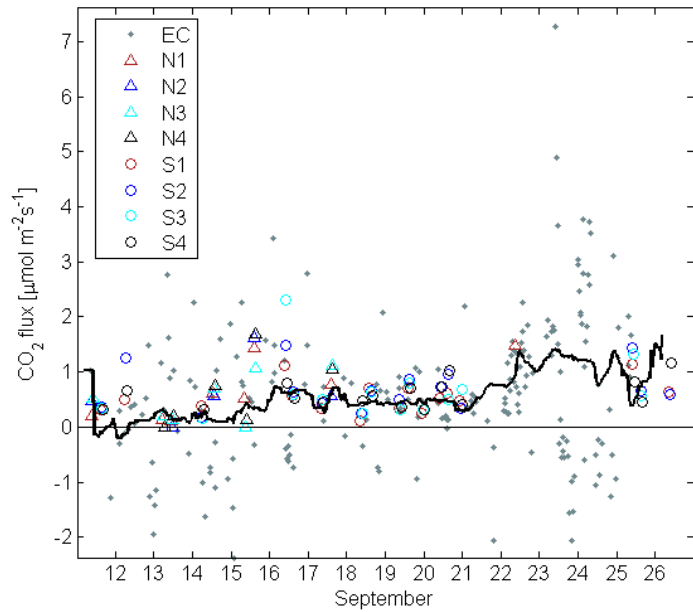
(b) CO$_2$ flux

Figure 9. Fluxes of a) CH$_4$ and b) CO$_2$. Chamber fluxes at different locations are shown in colorful circles and triangles, 30 min averages of eddy covariance flux are represented in gray dots. The black line is the moving average taken from the past and future 24 hours of EC measurements. Positive flux indicates emissions to the atmosphere and negative uptake of the gas.
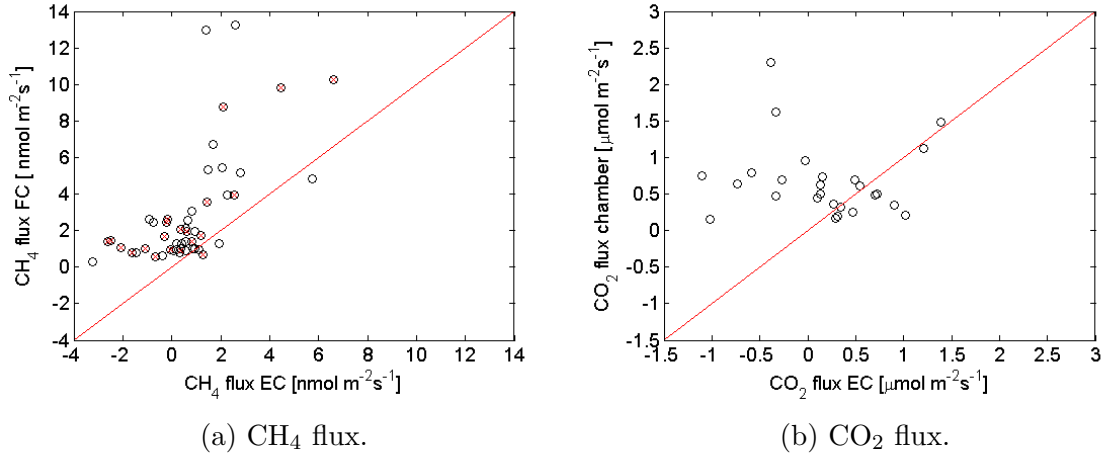
(a) CH$_4$ flux.

(b) CO$_2$ flux.

Figure 10. Comparison of a) CH$_4$ chamber flux and b) CO$_2$ chamber flux with 30 min average EC flux (x-axis). Red crosses in the CH$_4$ data represent measurements done near the shore. The red line represents the 1:1 reference line.

Cole and Caraco (1998) on the other hand seems to underestimate the flux most of the time. Fluxes are quite low during period 11.-22.9 when the lake is stratified, but they clearly increase after the mixing starts on 22.9. From this day on, the models by Tedford et al. (2014) and Heiskanen et al. (2014) agree better with EC measurements.

In Fig. 12 the CO$_2$ flux calculated according to Cole and Caraco (1998) is compared with averaged EC measurements before autumn mixing, 11.–22.9. Results indicate that the model mostly underestimates the flux. The model agrees better with EC measurements when the wind speed is higher than 2.5 ms^{-1}. This is an important result because so far most global estimates on lake GHG emissions are based on this technique and therefore they might be underestimated (Raymond et al., 2013; Tranvik et al., 2009). Heiskanen et al. (2014) found that the gas transfer velocity k did not depend on wind speed during stratified period in Lake Kuivajärvi until the wind speed reached values higher than 6 m/s. In this study, the wind speed did not reach as high values before mixing. After mixing started, the method gives clearly too low fluxes.

BLM fluxes from Tedford et al. (2014) and Heiskanen et al. (2014) are compared against average EC fluxes in Fig. 13. The comparison is much better (as the equations of linear fits indicate) because these models include buoyancy flux as another factor of controlling the gas exchange and the comparison is good even
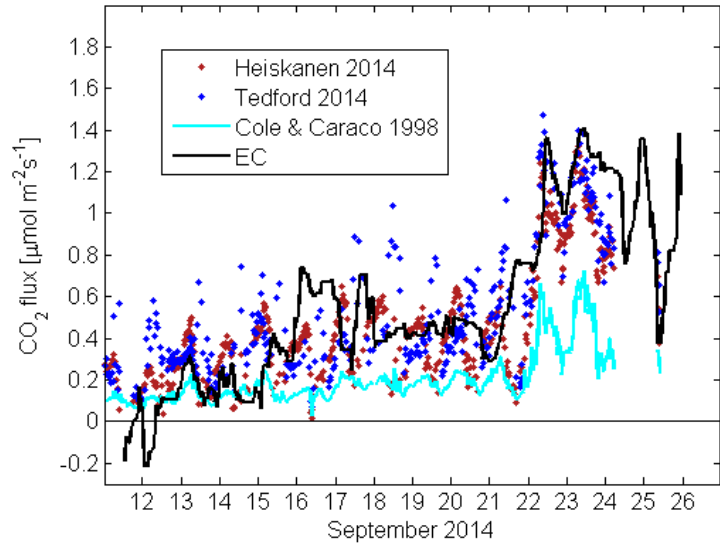
Figure 11. Time series comparison of EC measurements (black line, moving average of the past and future 24 hours of measurements) and BLM with transfer velocity calculated according to Eq. 17 (red), Eq. 14 (blue) and Eq. 11 (turquoise).
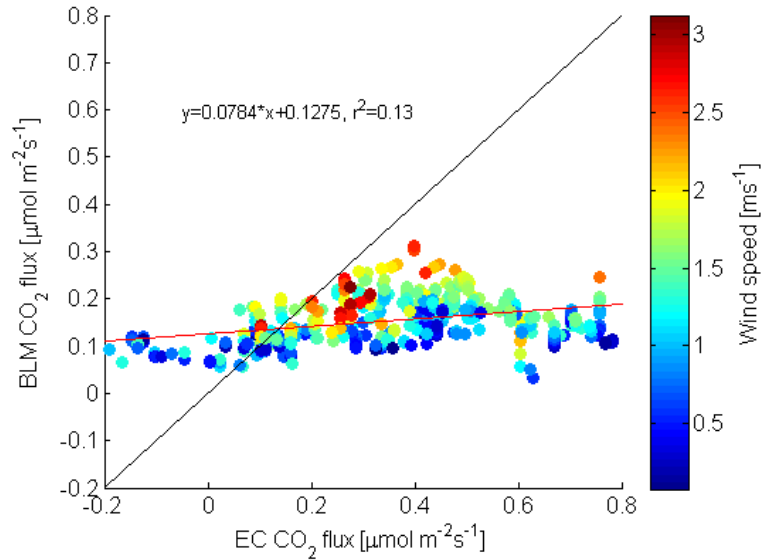

Figure 12. CO_2 flux determined by the boundary layer model with transfer velocity k calculated from Cole and Caraco, 1998 against EC flux measurements before autumn mixing, 11.–22.9. Different colors represent different wind speeds and the black line is the 1:1 reference line. The equation represents the linear fit of the measurements (red line).
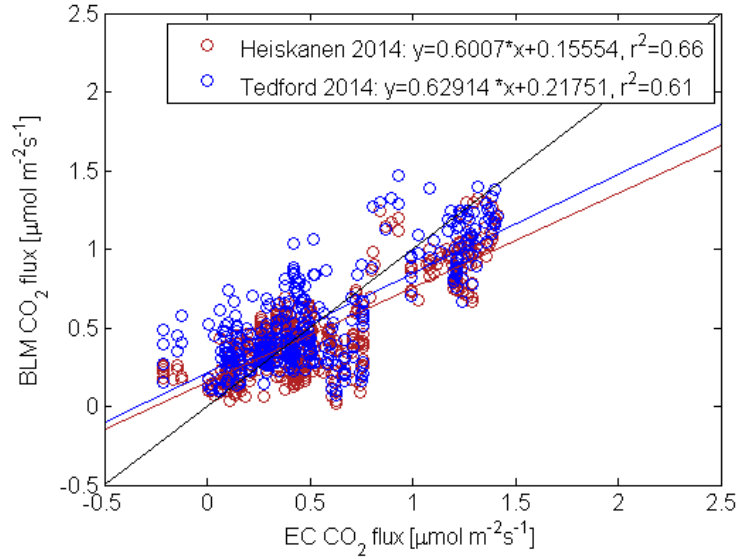
Figure 13. Comparison of EC moving averaged flux and BLM flux with transfer velocity calculated according to Heiskanen et al., 2014 (red) and Tedford et al., 2014 (blue). Black line is the 1:1 reference line.

when the mixing has started. The best fit against EC measurements is the k model by Heiskanen et al. (2014).

Again, BLM gives a flux estimate from a specific measurement point whereas EC gives an estimate over a larger area. As with FC and EC comparison, the conclusion is that these two methods give the flux estimates from different source areas and can be used for different types of studies.

4.4 Diurnal variation

Diurnal variations of both CH_4 and CO_2 fluxes and surface water concentration of CO_2 were studied separately before and after lake mixing started. FC fluxes were not measured continuously and thus diel variation is only calculated from EC and BLM measurements.

Diurnal variation of CH_4 flux measured with EC is shown in Fig. 14a. Before mixing, the fluxes are slightly negative during nighttime and positive during daytime. This kind of negative flux is probably due to generally low CH_4 fluxes, that are close to EC detection limit (Peltola et al., 2014). After mixing started, CH_4 flux shows a clear diurnal cycle with highest values reached at daytime/early evening (Fig. 14),
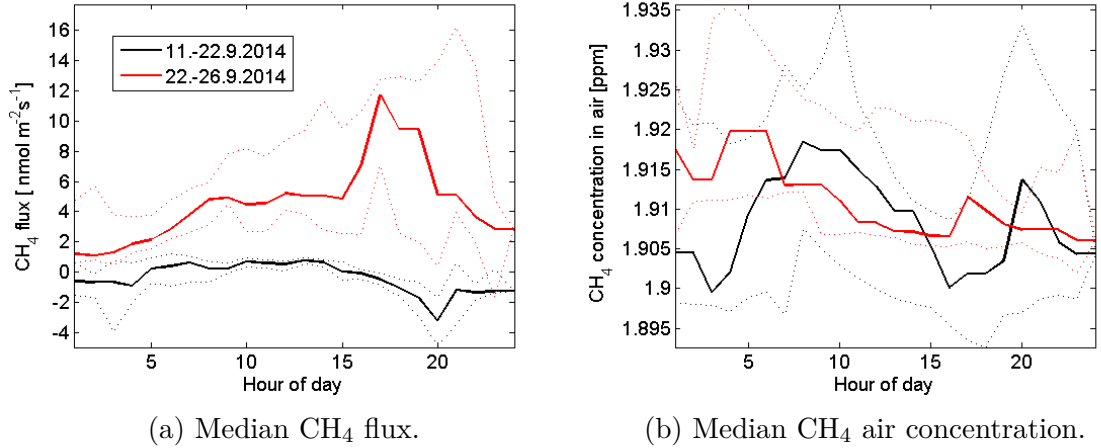
(a) Median CH$_4$ flux. (b) Median CH$_4$ air concentration.

Figure 14. Diurnal variation of CH$_4$ flux and air concentration before (black) and after (red) mixing started. Dashed curves are the 25th and 75th percentiles.

most likely due to wind induced mixing. This was the result also in Keller and Stallard (1994) but some studies have found an opposite cycle (Crill et al., 1988; Podgrajsek et al., 2014; Sahlée et al., 2014) with higher fluxes during night-time convection. Air concentration of CH$_4$ does not show any detectable diurnal cycle because the concentration changes are so small.

CO$_2$ flux variations measured with EC and BLM before and after mixing are examined in Figs. 15a and 15b. EC measurements do not show any diurnal variation before or after mixing while k_{Uw} shows lower daytime fluxes before mixing. BLM with k_{SR} on the other hand shows an opposite diurnal cycle and in k_{CC} there is no diurnal cycle. The diurnal cycle in k_{SR} is explained by the diurnal variation of friction velocity in the atmosphere. In this study, the aquatic friction velocity u_{*w} was calculated from the measured friction velocity in the atmosphere (Eq. 15). Water turbulence measurements (done with e.g. acoustic doppler velocimeter, ADV) would probably give more reliable results. Higher nighttime fluxes in Heiskanen et al. (2014) might be explained by nighttime convection, which is strongest at early morning when the lake surface has reached maximum cooling before the sunrise. Low daytime values are explained by photosynthetic binding of CO$_2$ (Vesala et al., 2006). After mixing started, diel variation in BLM fluxes disappears.
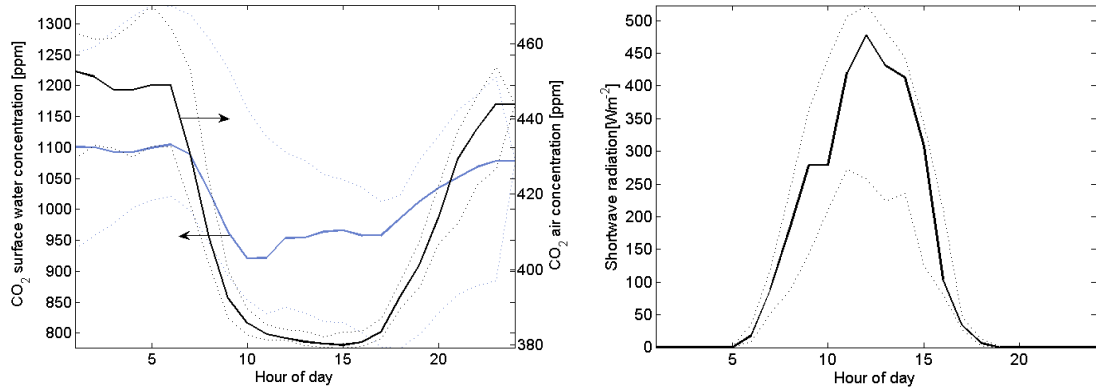
Air and surface water CO$_2$ concentrations show the clearest diurnal cycle (Fig. 16a), as expected. Photosynthesis of diatom is strong in the autumn due to turbulence in the water (Schindler and Fee, 1973) and this causes a clear decrease in the

39
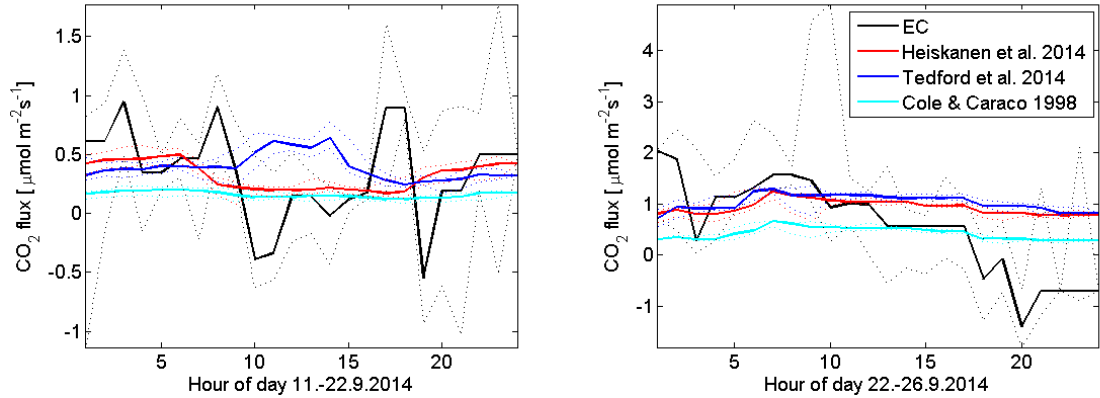
(a) Median CO_2 flux before mixing started.   (b) Median CO_2 flux during mixing period.

Figure 15. Diurnal variation of CO_2 flux measured with EC and BLM (a) before and (b) after lake turnover started. Dashed curves are the 25th and 75th percentiles.

surface water concentration in the daytime when the photosynthetic active radiation (PAR) has its highest values. PAR is directly proportional to incoming shortwave radiation and thus those two are comparable. After 5 pm the concentration starts to increase towards night. At this time of year, shortwave radiation is strongest at 12 am (Fig. 16b). After 5 pm, not much radiation reaches the surface and photosynthesis stops. This in turn increases the air and surface water concentrations of CO_2. Maximum values are gained at 6 am, after which decreasing starts again, right when shortwave radiation again increases i.e. sun rises. Concentration increase just before dusk and maximum values in early morning are also reported in Hari et al. (2008). Diurnal cycle of CO_2 concentration in air is very similar to water concentration variation, expect that there is a phase difference between these two with air concentration reaching its maximum and minimum before the water concentration. This might result from nighttime convection enhancing mixing that would bring gases from deeper waters to the surface. Convection starts in the late evening and stops in the morning when the surface water starts to warm. Really high air concentrations at nighttime are explained by the respiration of the surrounding forest and the stable nighttime conditions in the atmosphere that reduce mixing in the air. During daytime, mixing is strong in the atmosphere and wind usually along the lake and there is no advection from the forest. As a conclusion, CO_2 concentration in water is slower to react to variations in radiation than in air. It is also noteworthy, that the CO_2 concentration in air above the lake is much higher than the global av-

40

(a) Median CO_2 surface water concentration.

(b) Median short-wave radiation.

Figure 16. Diurnal variation of air and surface water CO_2 concentrations and incoming shortwave radiation measured at the raft. Dashed curves are the 25th and 75th percentiles.

erage atmospheric CO_2 concentration (Stocker et al., 2013), expect during daytime when the photosynthesis rate is highest.

5   Conclusions and final remarks

The main goal of this study was to compare three different greenhouse gas (GHG) flux measurement methods for carbon dioxide (CO_2) and methane (CH_4) fluxes. Measurements were done at Lake Kuivajärvi in Southern Finland during a 16 day field campaign in September 2014. Comparison included floating chamber (FC) method, water boundary layer model (BLM) with gas transfer velocity calculated according to three different studies and currently the most accurate flux measurement technique, the eddy covariance (EC) method. CO_2 and CH_4 fluxes were measured with both EC and FC, but BLM calculations only include CO_2 fluxes since CH_4 concentration in the surface water was not measured automatically. Manual FC measurements were conducted at different measurement points in the EC footprint area for studying spatial variability of fluxes. Measurement campaign was scheduled in the middle–end of September for catching the start of the lake autumn mixing period.

Lake Kuivajärvi started mixing in the end of the campaign, but mixing did not reach the bottom of the lake. Partial mixing however brought gases from hypolimnion to the surface and a clear increase in CH_4 flux measured both with EC and FC was detected. CO_2 flux measured with EC and BLM methods also showed a clear increase, whereas no notable increase was detected with FC measurements. No significant spatial variability was detected with FC CO_2 measurements. FC CH_4 fluxes on the other hand showed some notably higher fluxes measured near the shore.

FC CH_4 fluxes were higher than EC fluxes presumably due to local upwelling occasions. CH_4 flux over Lake Kuivajärvi is generally quite small and close to the EC detection limit. CO_2 FC fluxes were mostly higher than EC, but the comparison was not as clear as for CH_4. This was also a result in other recent comparison study (Podgrajsek et al., 2014).

The Cole and Caraco (1998) BLM was underestimating the fluxes most of the time when compared with EC, whereas BLM fluxes from Tedford et al. (2014) and Heiskanen et al. (2014) showed better agreement with EC measurements. The best approximation for gas transfer velocity was from the most recent study by Heiskanen et al. (2014). Tedford et al. (2014) would probably give a better estimate if the water

friction velocity was measured directly from water and not derived from atmospheric measurements. Better agreement between EC and BLM methods was found after the lake started mixing, when the fluxes were higher. Also wind speed at this time was higher and might partly cause this.

Difference in the fluxes measured with all three methods is caused by the very different source areas that these methods represent. EC measures fluxes over a large footprint area while BLM and FC fluxes represent spot measurements. Thus, these methods can be used for different measurement purposes. Global estimates calculated according to Cole and Caraco (1998) are markedly underestimates.

One aim was also to study diurnal variations of the fluxes and air and surface water concentrations. Diel cycle in CH_4 flux was found with higher values during daytime in the mixing period. High daytime flux is most probably due to wind-induced mixing, which was also a result in Keller and Stallard (1994). Before mixing, CO_2 flux in turn had a diel cycle with low values in the daytime due to photosynthesis when measured with Heiskanen et al. (2014) BLM method. Tedford et al. (2014) showed an opposite cycle most probably due to lack of turbulence data from the water. EC measurements did not show a diurnal cycle in CO_2 flux.

So far there are only a few method comparison studies about GHG flux measurements over lakes, especially including all three methods and for both CO_2 and CH_4. Results from these studies are not consistent and thus these comparisons should be further developed. Models for lake heat exchange have already been produced but tested models for GHG exchange are still lacking. In the future, it would be interesting to use measurements in different lakes and seasons to improve BLM method for better GHG exchange modelling.

References

Åberg, J., M. Jansson, and A. Jonsson (2010): "Importance of water temperature and thermal stratification dynamics for temporal variation of surface water CO2 in a boreal lake", *Journal of Geophysical Research: Biogeosciences (2005–2012)* **115**.G2.

Anderson, D. E., R. G. Striegl, D. I. Stannard, C. M. Michmerhuizen, T. A. McConnaughey, and J. W. LaBaugh (1999): "Estimating lake-atmosphere CO˜ 2 exchange", *Limnology and oceanography* **44**, 988–1001.

Aubinet, M., T. Vesala, and D. Papale (2012): *Eddy covariance: a practical guide to measurement and data analysis*, Springer Science & Business Media.

Bastviken, D., J. Cole, M. Pace, and L. Tranvik (2004): "Methane emissions from lakes: Dependence of lake characteristics, two regional assessments, and a global estimate", *Global biogeochemical cycles* **18**.4.

Bastviken, D., A. L. Santoro, H. Marotta, L. Q. Pinho, D. F. Calheiros, P. Crill, and A. Enrich-Prast (2010): "Methane emissions from Pantanal, South America, during the low water season: toward more comprehensive sampling", *Environmental science & technology* **44**.14, 5450–5455.

Bastviken, D., L. J. Tranvik, J. A. Downing, P. M. Crill, and A. Enrich-Prast (2011): "Freshwater methane emissions offset the continental carbon sink", *Science* **331**.6013, 50–50.

Bastviken, D., I. Sundgren, S. Natchimuthu, H. Reyier, and M. Gålfalk (2015): "Technical Note: Cost-efficient approaches to measure carbon dioxide (CO 2) fluxes and concentrations in terrestrial and aquatic environments using mini loggers", *Biogeosciences Discussions* **12**.3, 2357–2380.

Bernstein, L., P. Bosch, O. Canziani, Z.n Chen, R. Christ, O. Davidson, W. Hare, S. Huq, D. Karoly, and V. Kattsov (2007): "IPCC, 2007: climate change 2007: synthesis report. Contribution of working groups I", *II and III to the Fourth Assessment Report of the Intergovernmental Panel on Climate Change. Intergovernmental Panel on Climate Change, Geneva.*

Chanton, J. P. and G. J. Whiting (1995): "Trace gas exchange in freshwater and coastal marine environments: ebullition and transport by plants", *Biogenic trace gases: measuring emissions from soil and water*, 98–125.

Cole, J. J. and N. F. Caraco (1998): "Atmospheric exchange of carbon dioxide in a low-wind oligotrophic lake measured by the addition of SF6", *Limnology and Oceanography* **43**.4, 647–656.

Cole, J. J., N. F. Caraco, G. W. Kling, and T. K. Kratz (1994): "Carbon dioxide supersaturation in the surface waters of lakes", *Science (New York, N.Y.)* **265**.5178, 1568–1570.

Cole, J. J., Y. T. Prairie, N. F. Caraco, W. H. McDowell, L. J. Tranvik, R. G. Striegl, C. M. Duarte, P. Kortelainen, J. A. Downing, and J. J. Middelburg (2007): "Plumbing the global carbon cycle: integrating inland waters into the terrestrial carbon budget", *Ecosystems* **10**.1, 172–185.

Crill, P., K. Bartlett, J. Wilson, D Sebacher, R. Harriss, J. Melack, S. MacIntyre, L. Lesack, and L. Smith-Morrill (1988): "Tropospheric methane from an Amazonian floodplain lake", *Journal of Geophysical Research* **93**.D2, 1564–1570.

Deacon, E. L. (1977): "Gas transfer to and across an air-water interface", *Tellus A* **29**.4.

Duc, Nguyen Thanh, Samuel Silverstein, Lars Lundmark, Henrik Reyier, Patrick Crill, and David Bastviken (2012): "Automated flux chamber for investigating gas flux at water–air interfaces", *Environmental science & technology* **47**.2, 968–975.

Eugster, W., G. Kling, T. Jonas, J. P. McFadden, A. Wüest, S. MacIntyre, and F. S. Chapin (2003): "CO2 exchange between air and water in an Arctic Alaskan and midlatitude Swiss lake: Importance of convective mixing", *Journal of Geophysical Research: Atmospheres (1984–2012)* **108**.D12.

Eugster, W., T. DelSontro, and S. Sobek (2011): "Eddy covariance flux measurements confirm extreme CH4 emissions from a Swiss hydropower reservoir and resolve their short-term variability", *Biogeosciences* **8**.9, 2815–2831.

Foken, Th. and B. Wichura (1996): "Tools for quality assessment of surface-based flux measurements", *Agricultural and forest meteorology* **78**.1, 83–105.

Godwin, C. M., P. J. McNamara, and C. D. Markfort (2013): "Evening methane emission pulses from a boreal wetland correspond to convective mixing in hollows", *Journal of Geophysical Research: Biogeosciences* **118**.3, 994–1005.

Hanson, P. C., A. I. Pollard, D. L. Bade, K. Predick, S. R. Carpenter, and J. A. Foley (2004): "A model of carbon evasion and sedimentation in temperate lakes", *Global Change Biology* **10**.8, 1285–1298.

Happell, J. D. and J. P. Chanton (1993): "Carbon remineralization in a north Florida swamp forest: effects of water level on the pathways and rates of soil organic matter decomposition", *Global Biogeochemical Cycles* **7**.3, 475–490.

Hari, P., J. Pumpanen, J. Huotari, P. Kolari, J. Grace, T. Vesala, and A. Ojala (2008): "High-frequency measurements of productivity of planktonic algae using rugged nondispersive infrared carbon dioxide probes", *Limnology and Oceanography: Methods* **6**.8, 347–354.

Heiskanen, J. J., I. Mammarella, S. Haapanala, J. Pumpanen, T. Vesala, S. MacIntyre, and A. Ojala (2014): "Effects of cooling and internal wave motions on gas transfer coefficients in a boreal lake", *Tellus B* **66**.

Horst, T. W. (1997): "A simple formula for attenuation of eddy fluxes measured with first-order-response scalar sensors", *Boundary-Layer Meteorology* **82**.2, 219–233.

Houghton, J., Y. Ding, D. J. Griggs, M. Noguer, P. J. Van der Linden, X. Dai, K. Maskell, and C. A. Johnson (2001): "IPCC 2001: Climate Change 2001", *The Climate change Contribution of Working Group I to the Third Assessment Report of the Intergovemmental Panel on Climate Change* **159**.

Huotari, J., A. Ojala, E. Peltomaa, J. Pumpanen, P. Hari, and T. Vesala (2009): "Temporal variations in surface water CO2 concentration in a boreal humic lake based on high-frequency measurements", *Boreal Environment Research* **14**, 48–60.

Huotari, J., A. Ojala, E. Peltomaa, A. Nordbo, S. Launiainen, J. Pumpanen, T. Rasilo, P. Hari, and T. Vesala (2011): "Long term direct CO2 flux measurements over a boreal lake: Five years of eddy covariance data", *Geophysical Research Letters* **38**.18.

Imberger, J. (1985): "The diurnal mixed layer1", *Limnology and oceanography* **30**.4, 737–770.

Kaimal, J. C. and J. J. Finnigan (1994): "Atmospheric boundary layer flows: their structure and measurement".

Keller, M. and R. F. Stallard (1994): "Methane emission by bubbling from Gatun Lake, Panama", *Journal of Geophysical Research: Atmospheres (1984–2012)* **99**.D4, 8307–8319.

LI-COR: *LI-7200 Enclosed CO_2/H2O Gas Analyzer Instruction manual*, LI-COR, 4647 Superior Street P.O. Box 4425 Lincoln, Nebraska USA 68504-0425.

Livingston, G. P. and G. L. Hutchinson (1995): "Enclosure-based measurement of trace gas exchange: applications and sources of error", *Biogenic trace gases: measuring emissions from soil and water*, 14–51.

MacIntyre, S., R. Wanninkhof, and J.P. Chanton (1995): "Trace gas exchange across the air-water interface in freshwater and coastal marine environments", *Biogenic trace gases: Measuring emissions from soil and water* **5297**.

MacIntyre, S., A. Jonsson, M. Jansson, J. Åberg, D. E. Turney, and S. D. Miller (2010): "Buoyancy flux, turbulence, and the gas transfer coefficient in a stratified lake", *Geophysical Research Letters* **37**.24.

Mammarella, I., S. Launiainen, T. Grönholm, P.i Keronen, J. Pumpanen, Üllar Rannik, and T. Vesala (2009): "Relative humidity effect on the high-frequency attenuation of water vapor flux measured by a closed-path eddy covariance system", *Journal of Atmospheric and Oceanic Technology* **26**.9, 1856–1866.

Mammarella, I., A. Nordbo, Ü. Rannik, S. Haapanala, J. Levula, H. Laakso, A. Ojala, O. Peltola, J. Heiskanen, and J. Pumpanen (2015): "Carbon dioxide and energy fluxes over a small boreal lake in Southern Finland", *Journal of Geophysical Research: Biogeosciences.*

McGillis, W. R., J. B. Edson, C. J. Zappa, J. D. Ware, S. P. McKenna, E. A. Terray, J. E. Hare, C. W. Fairall, W. Drennan, and M. Donelan (2004): "Air-sea CO2 exchange in the equatorial Pacific", *Journal of Geophysical Research: Oceans (1978–2012)* **109**.C8.

Ojala, A., J. L. Bellido, T. Tulonen, P. Kankaala, and J. Huotari (2011): "Carbon gas fluxes from a brown-water and a clear-water lake in the boreal zone during a summer with extreme rain events", *Limnology and Oceanography* **56**.1, 61–76.

Peltola, O., A. Hensen, C. Helfter, L. Belelli Marchesini, F. C. Bosveld, W. C. M. Van Den Bulk, J. A. Elbers, S. Haapanala, J. Holst, T. Laurila, et al. (2014): "Evaluating the performance of commonly used gas analysers for methane eddy covariance flux measurements: the InGOS inter-comparison field experiment", *Biogeosciences Discussions* **11**.1, 797–852.

Podgrajsek, E., E. Sahlée, D. Bastviken, J. Holst, A. Lindroth, Tranvik L., and A. Rutgersson (2014): "Comparison of floating chamber and eddy covariance measurements of lake greenhouse gas fluxes", *Biogeosciences Discussions* **11**, 4225–4233.

Raymond, P. A., J. Hartmann, R. Lauerwald, S. Sobek, C. McDonald, M. Hoover, D. Butman, R. Striegl, E. Mayorga, and C. Humborg (2013): "Global carbon dioxide emissions from inland waters", *Nature* **503**.7476, 355–359.

Read, J. S., D. P. Hamilton, A. R. Desai, K. C. Rose, S. MacIntyre, J. D. Lenters, R. L. Smyth, P. C. Hanson, J. J. Cole, and P. A. Staehr (2012): "Lake-size dependency of wind shear and convection as controls on gas exchange", *Geophysical Research Letters* **39**.9.

Sahlée, E., A. Rutgersson, E. Podgrajsek, and H. Bergström (2014): "Influence from surrounding land on the turbulence measurements above a lake", *Boundary-layer meteorology* **150**.2, 235–258.

Schindler, D. W. and E. J. Fee (1973): "Diurnal variation of dissolved inorganic carbon and its use in estimating primary production and CO2 invasion in Lake 227", *Journal of the Fisheries Board of Canada* **30**.10, 1501–1510.

Schubert, C. J., T. Diem, and W. Eugster (2012): "Methane emissions from a small wind shielded lake determined by eddy covariance, flux chambers, anchored funnels, and boundary model calculations: a comparison", *Environmental science & technology* **46**.8, 4515–4522.

Stocker, T. F., D. Qin, G. K. Plattner, M. Tignor, S. K. Allen, J. Boschung, A. Nauels, Y. Xia, B. Bex, and B. M. Midgley (2013): "IPCC, 2013: climate change 2013: the physical science basis. Contribution of working group I to the fifth assessment report of the intergovernmental panel on climate change".

Stull, R. B. (1988): *An introduction to boundary layer meteorology*, vol. 13, Springer Science & Business Media.

Tedford, E. W., S. MacIntyre, S. D. Miller, and M. J. Czikowsky (2014): "Similarity scaling of turbulence in a temperate lake during fall cooling", *Journal of Geophysical Research: Oceans* **119**.8, 4689–4713.

Tranvik, L. J., J. A. Downing, J. B. Cotner, S. A. Loiselle, R. G. Striegl, T. J. Ballatore, P. Dillon, K. Finlay, K. Fortino, and L. B. Knoll (2009): "Lakes and reservoirs as regulators of carbon cycling and climate", *Limnology and Oceanography* **54**.6part2, 2298–2314.

Vachon, D., Y. T. Prairie, and J. J. Cole (2010): "The relationship between near-surface turbulence and gas transfer velocity in freshwater systems and its implications for floating chamber measurements of gas exchange", *Limnology and Oceanography* **55**.4, 1723–1732.

Vesala, T., J. Huotari, Ü. Rannik, T. Suni, S. Smolander, A. Sogachev, S. Launiainen, and A. Ojala (2006): "Eddy covariance measurements of carbon exchange and latent and sensible heat fluxes over a boreal lake for a full open water period", *Journal of Geophysical Research: Atmospheres (1984–2012)* **111**.D11.

Vickers, D. and L. Mahrt (1997): "Quality control and flux sampling problems for tower and aircraft data", *Journal of Atmospheric and Oceanic Technology* **14**.3, 512–526.

Wetzel, R. G. (2001): *Limnology: lake and river ecosystems*, Gulf Professional Publishing.

Zappa, C. J., W. R. McGillis, P. A. Raymond, J. B. Edson, E. J. Hintsa, H. J. Zemmelink, J. Dacey, and D. T. Ho (2007): "Environmental turbulent mixing controls on air-water gas exchange in marine and aquatic systems", *Geophysical Research Letters* **34**.10.